

Probing Ferroelectricity, Charge Density Wave Dynamics, and Magnetism with Submicron X-ray Diffraction

Paul G. Evans

Department of Materials Science and Engineering

University of Wisconsin, Madison

evans@engr.wisc.edu

College of Engineering
University of Wisconsin-Madison



APS SAC
Microbeam Review
January 21, 2004

Outline

- Brief Introduction to Microbeam Experiments at Sector 7 of the APS
- Overview: Physical Phenomena and Motivation
- In Depth: Polarization Switching and Fatigue in PZT Thin Films, Magnetic Domain Evolution in Antiferromagnetic Chromium
- Conclusions, Future Directions

MHATT-CAT Sector 7

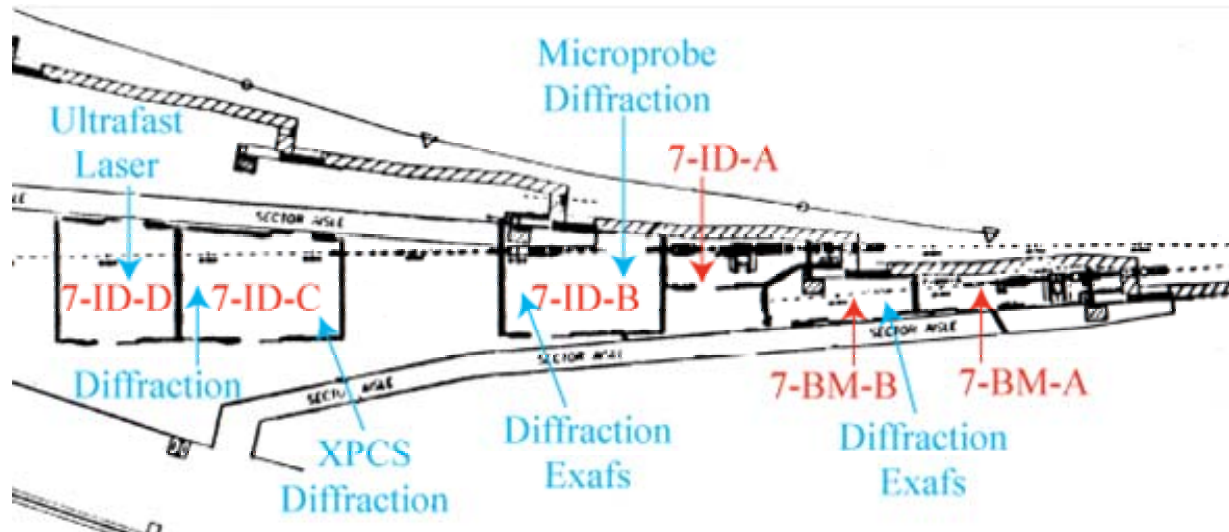
Center for Real-time X-ray Studies



Unique Capabilities:

- *Ultrafast Laser Facility*
- *Staff Expertise in Ultrafast Optics and X-ray Science, Diffraction, Scattering, and Spectroscopy*
- *White Beam Diffraction with Submicron Focusing with G. Ice-style Mirrors*
- *Small Angle Scattering/XPCS with Fast CCD Direct Detection*

MHATT-CAT's mission:
To develop a productive, open-access center for world-class research in x-ray science exploiting the unique characteristics of the APS, especially timing and brilliance.



Microbeam General User Research at Sector 7



- **Relaxation dynamics of magnetic polymers using XPCS (collaboration with Ford Research, Dearborn, MI)**
- Micro-fluorescence mapping of mineral intrusions (Dan Core, Geosciences Dept., Michigan)
- **Development of Li-metal x-ray lenses (Nino Pereira, Ecopulse Inc., Fairfax, VA)**
- Studies of core excitations in Kr microjets (Linda Young, ANL)
- Doped magnetic semiconductors (Frank Tsui, U. of North Carolina, Y. Chu, APS)

DYNAMICS IN MAGNETORHEOLOGICAL ELASTOMERS

William F. Schlotter, Codrin Cionca, Sirinivas S. Paruchuri, Jevne B. Cunningham, Eric Dufresne, Steve B. Dierker, Dohn Arms and Roy Clarke

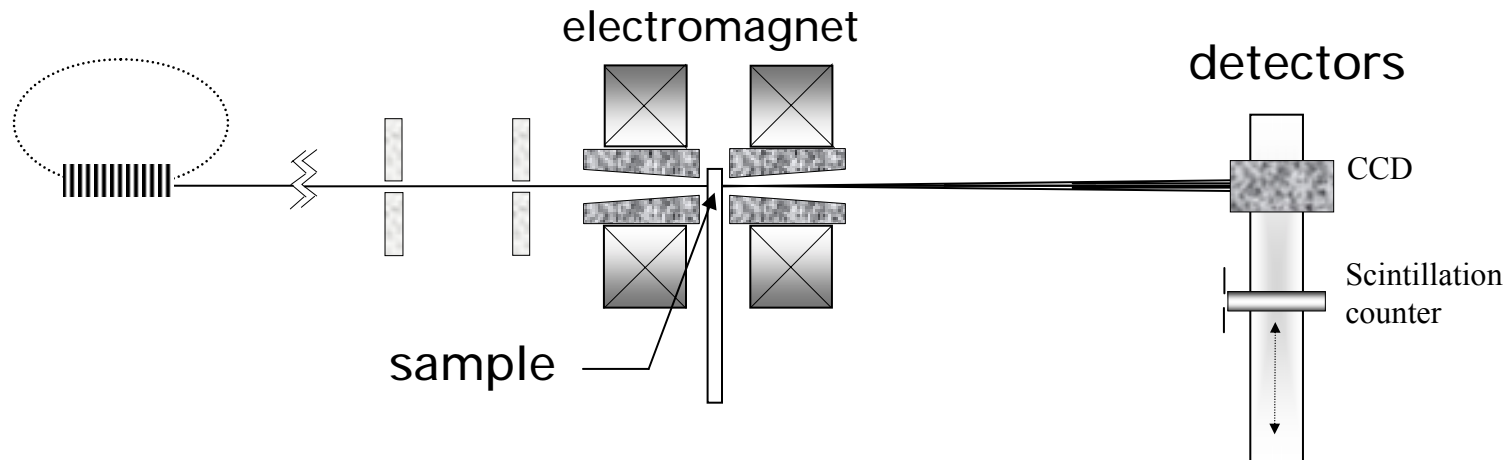
University of Michigan, Ann Arbor

John M. Ginder and Mark E. Nichols

Ford Motor Company, Research Laboratory, Dearborn, MI

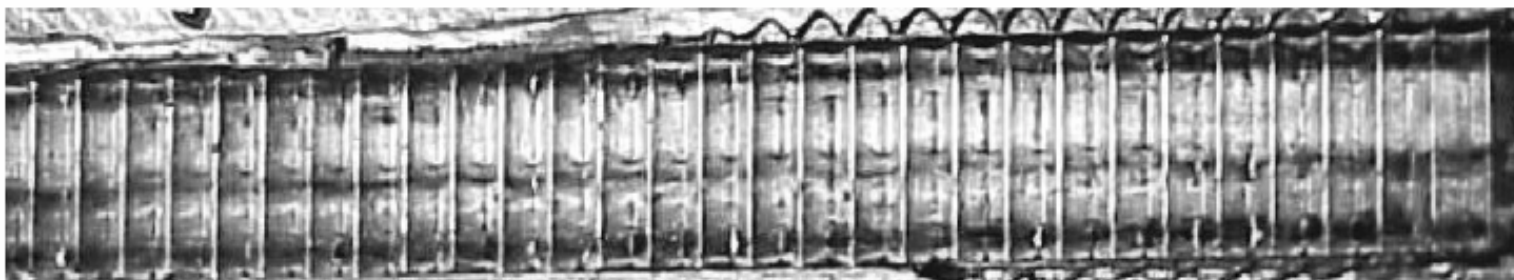


Coherent small angle scattering.



**MR sample is rigidly mounted while
direction of magnetic field is alternated**

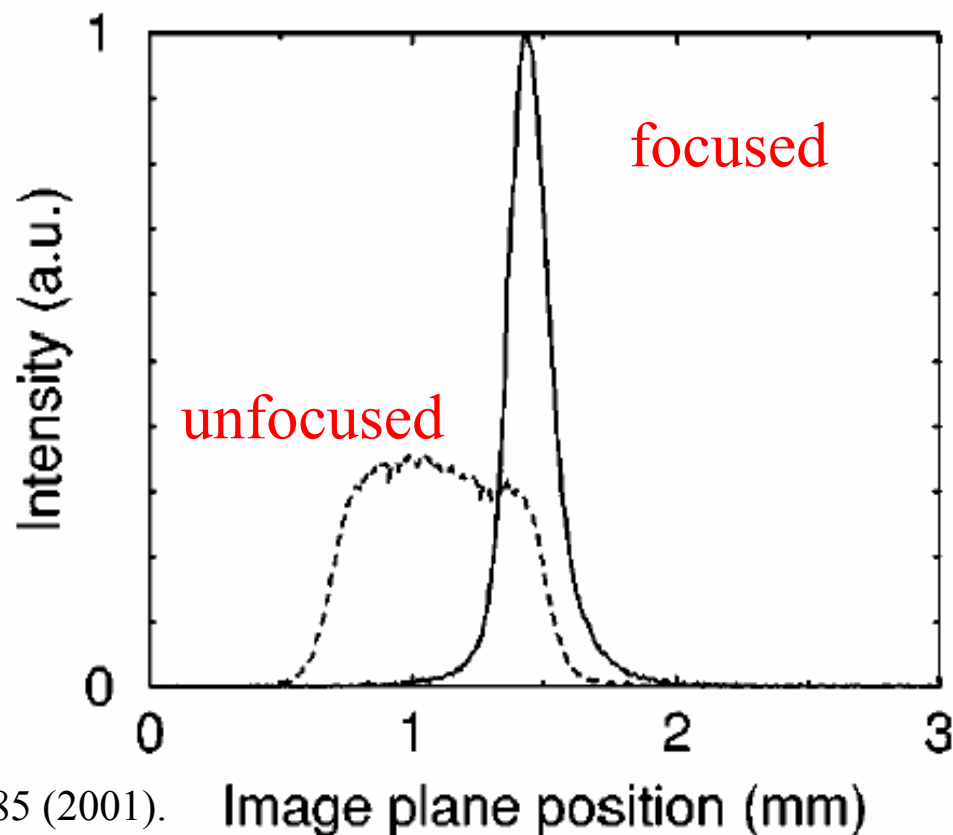
LITHIUM REFRACTIVE LENSES



Sawtooth Li Lens

Sawtooth and Parabolic Lithium Lenses

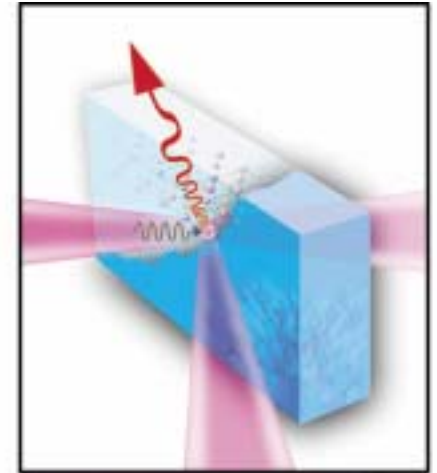
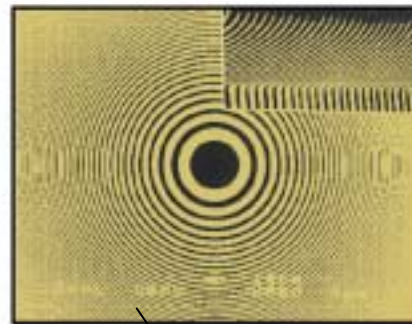
Recent results:
flux gain ~ 40
spot size $\sim 20 \mu\text{m}$



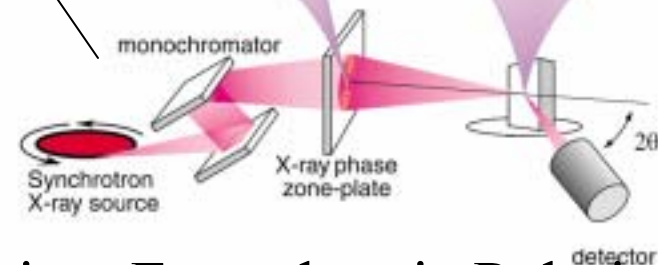
E. M. Dufresne, *et al.*, Appl. Phys. Lett. **79**, 4085 (2001).

N. R. Pereira, *et al.*, Rev. Sci. Instrum. **75** 37 (2004).

X-ray Microdiffraction as a Tool for Physics and Materials Science



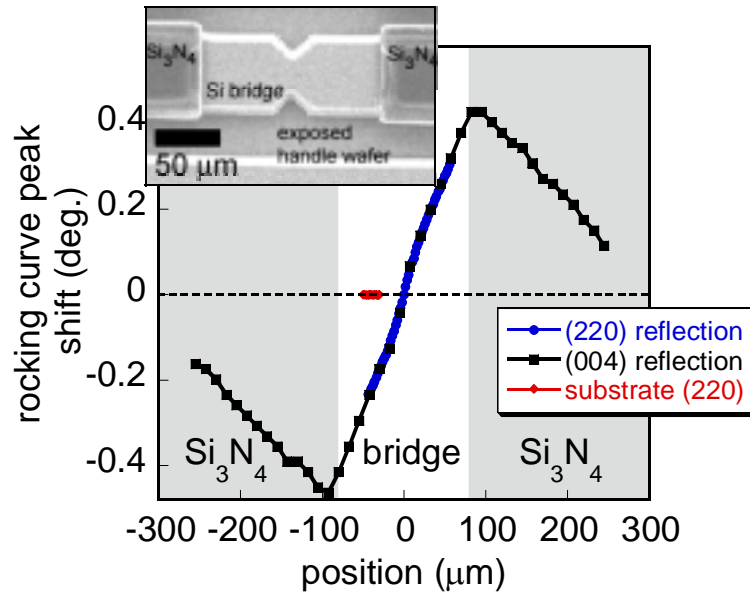
- 6 to 30 keV
- 10^{10} ph/s/0.01%BW
- Minimum spot (APS, sector 2)-
 $0.15 \times 0.15 \mu\text{m}^2$



Contrast from: Diffraction, Composition, Ferroelectric Polarization, Magnetization.

Problems with existing techniques: time resolution, electrodes, quantification.

Submicron Science with X-ray Diffraction



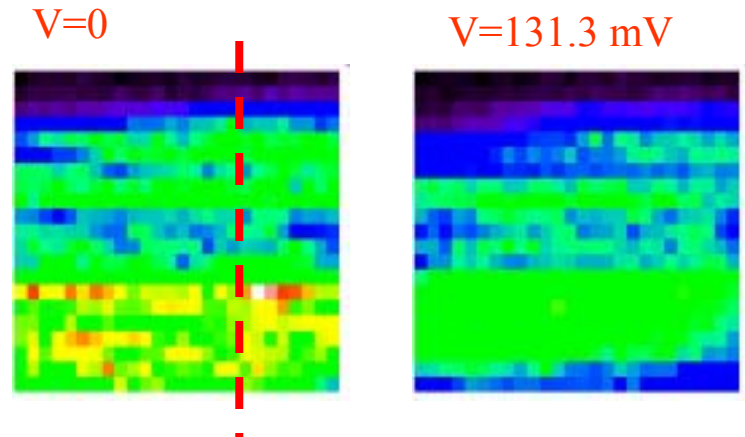
Strain in MEMS-inspired substrates
for SiGe epitaxial growth.

(Sector 2)

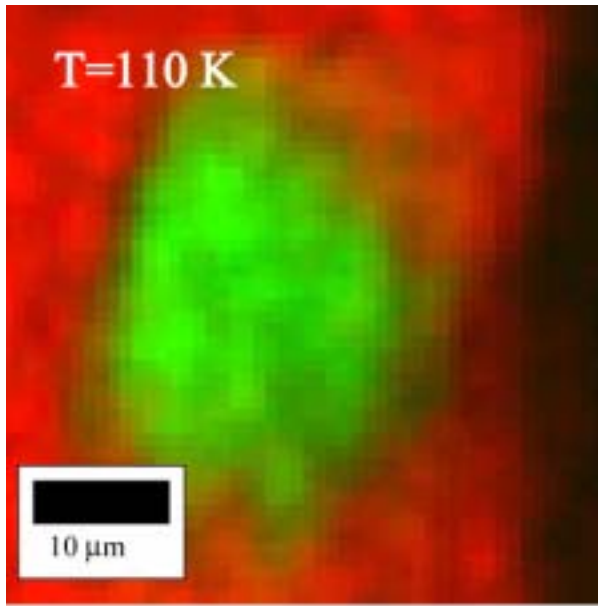
With B. Lai, Z. Cai (APS),
P. Rugheimer, and M. Lagally (U. Wisc.)
(P. G. Evans *et al.*, submitted, Jan. 2004)

Charge density wave
dynamics in NbSe₃ (Sector 2)

With R. Thorne (Cornell U.)



Submicron Science

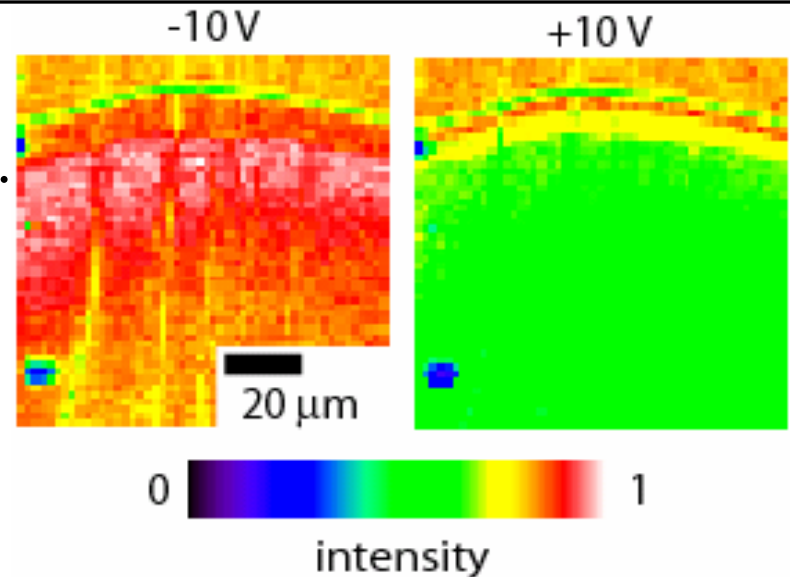


Spin density wave antiferromagnetism in Cr
(Sector 2)

With E. Isaacs, B. Lai, Z. Cai (ANL)
(P. G. Evans *et al.*, Science 2002)

Polarization reversal and piezoelectric distortion in ferroelectric PZT thin films.
(Sector 7)

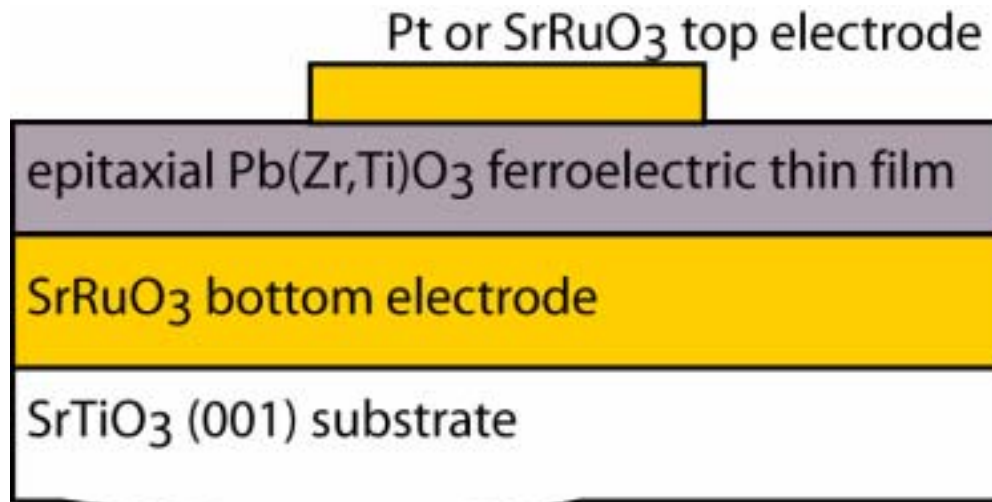
With C.-B. Eom, (U. Wisc) and E. Dufresne (U. Mich/Sector 7)
(D.-H. Do *et al.*, submitted, Nov. 2003)



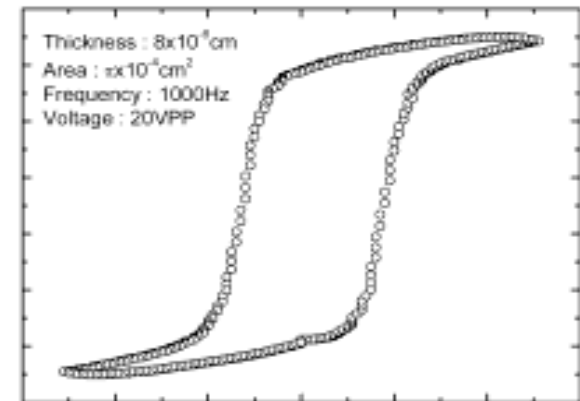
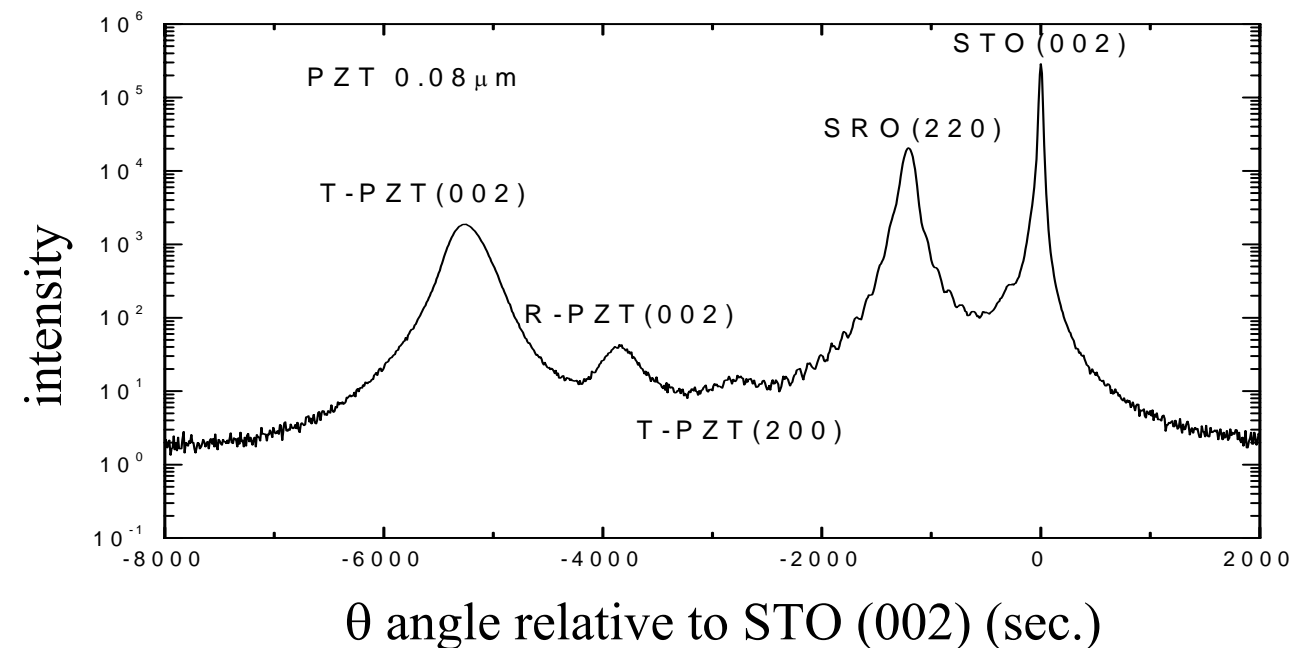
Outline

- Brief Introduction to Microbeam Experiments at Sector 7 of the APS
- Overview: Physical Phenomena and Motivation
- In Depth: Polarization Switching and Fatigue in PZT Thin Films, Magnetic Domain Evolution in Antiferromagnetic Chromium
- Conclusions, Future Directions

Epitaxial PZT Thin Film Capacitors

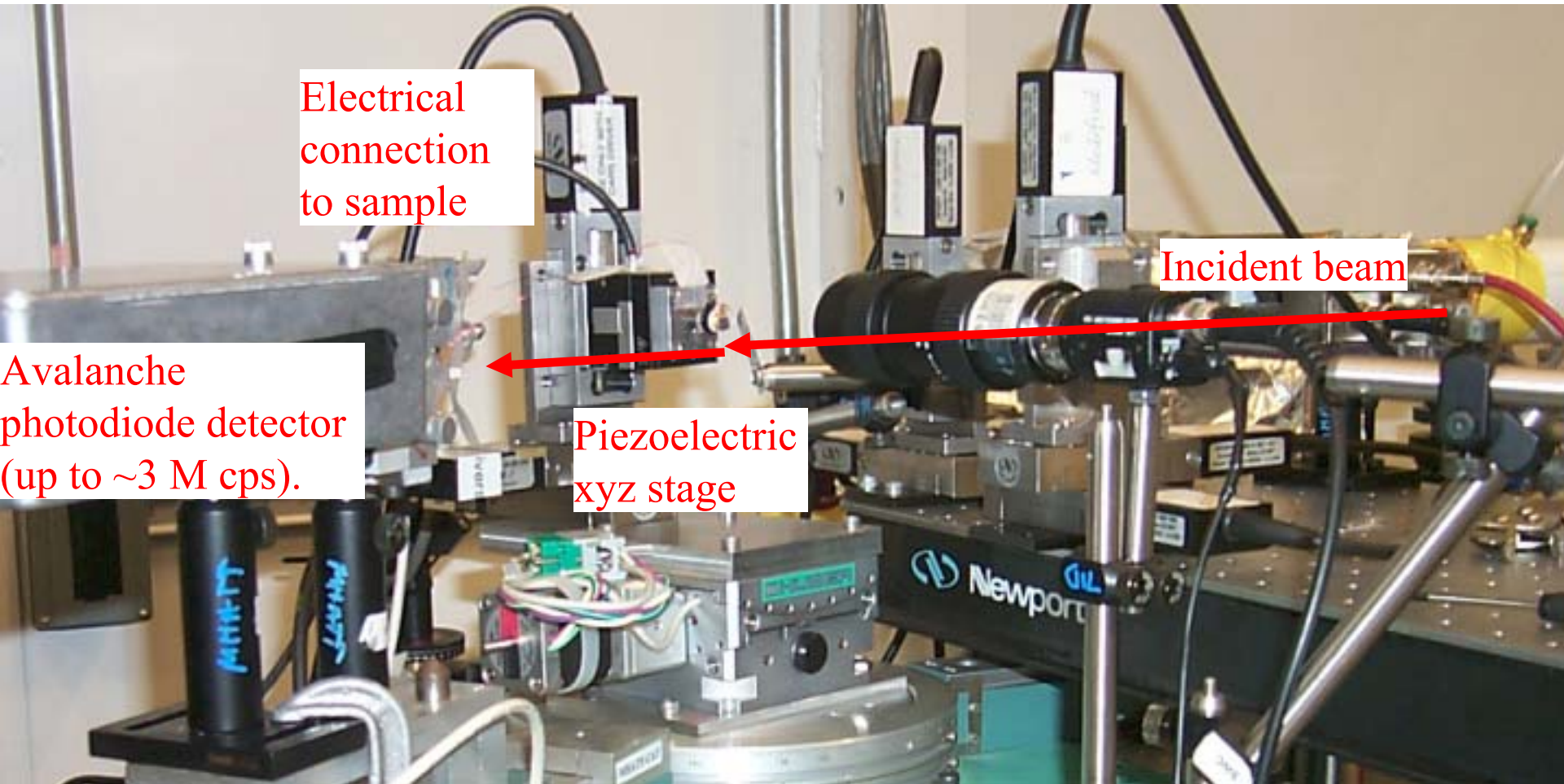


tetragonal PbZr_{1-x}Ti_xO₃
 $x=0.55$
 80 nm or 160 nm PZT
 thickness



$$2 P_r \approx 95 \mu\text{C}/\text{cm}^2$$

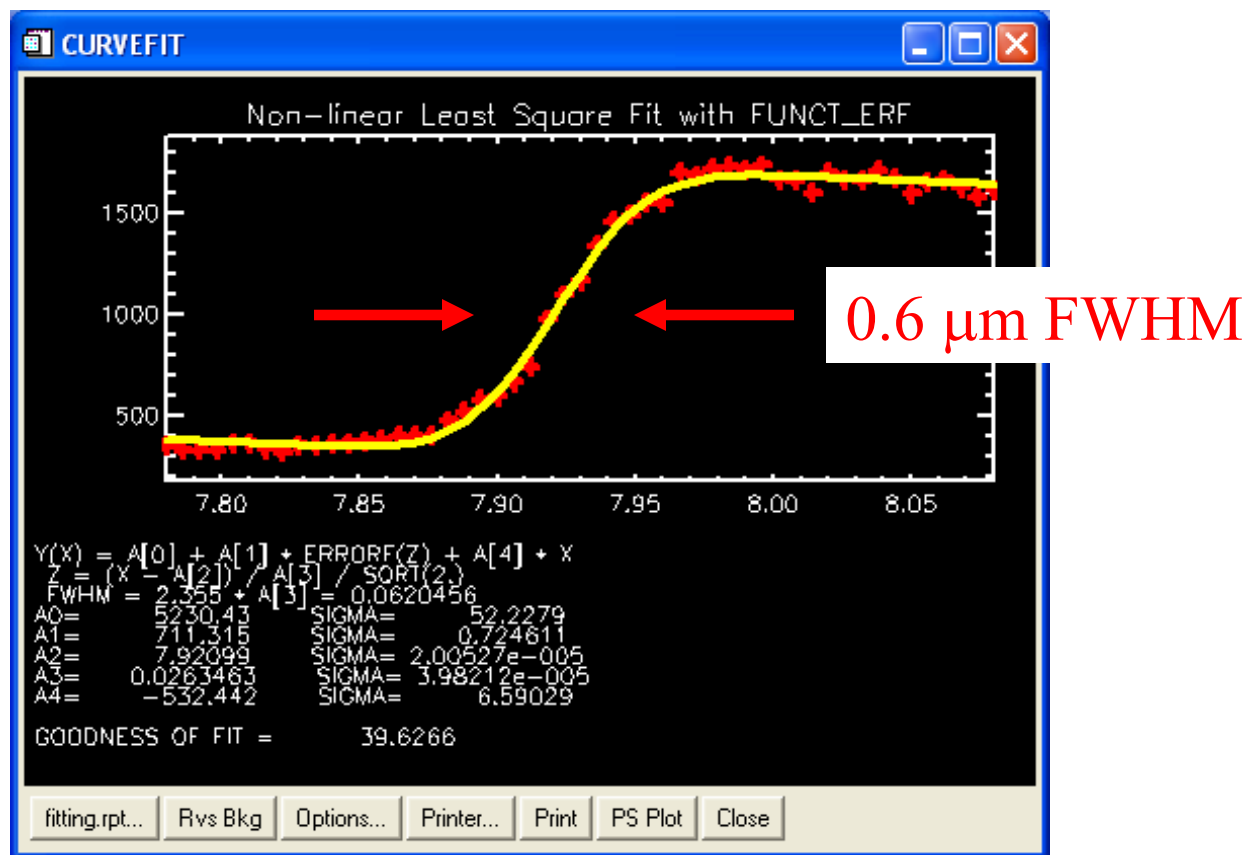
Time Resolved Microdiffraction with Zone Plate Optics at Sector 7



Use avalanche photodiode with multichannel scaler to time-resolve the diffraction signal during voltage pulses.

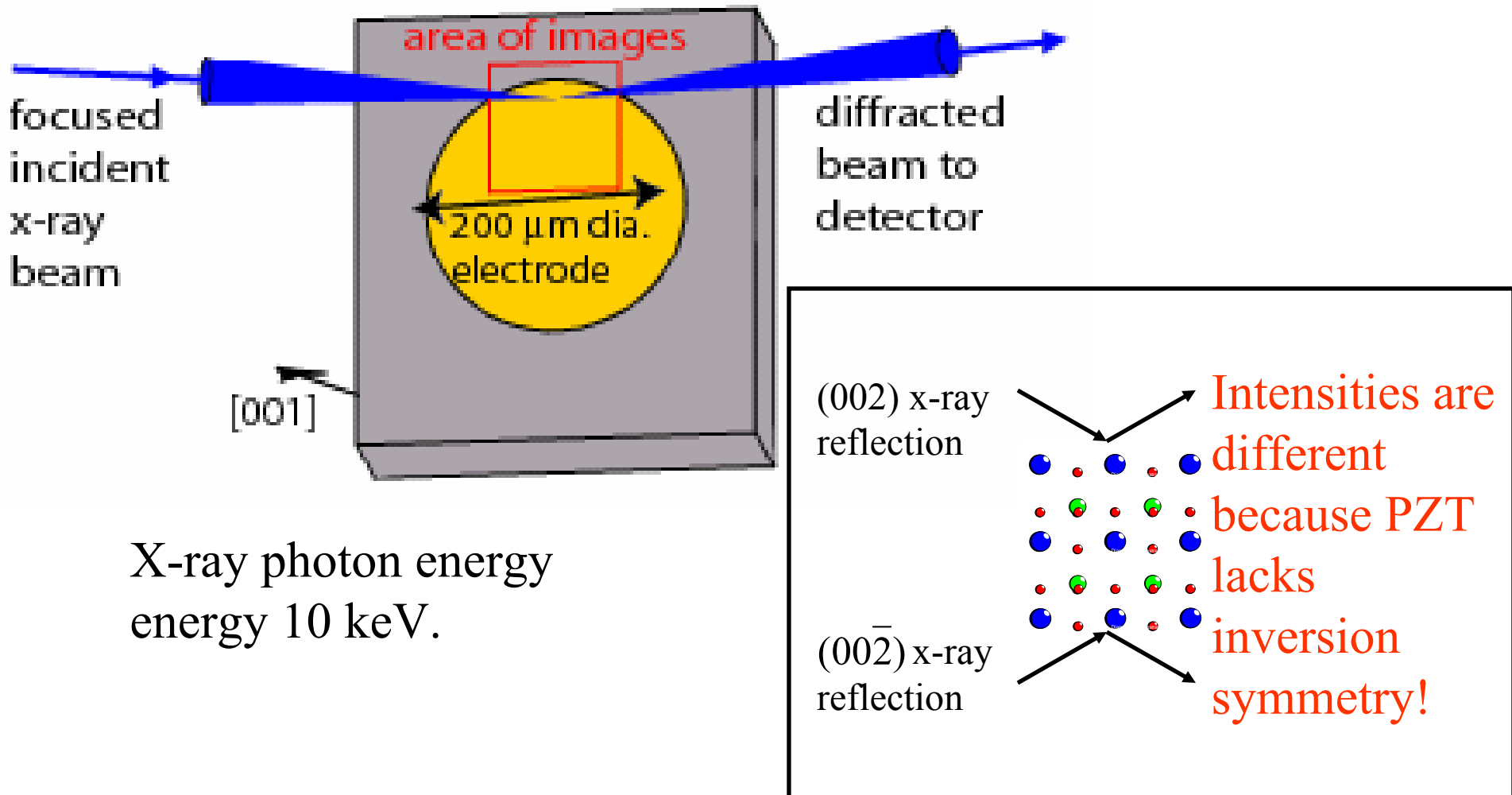
Aside: Spatial Resolution at Sector 7

Spatial Resolution:
Knife Edge
Fluorescence Scan

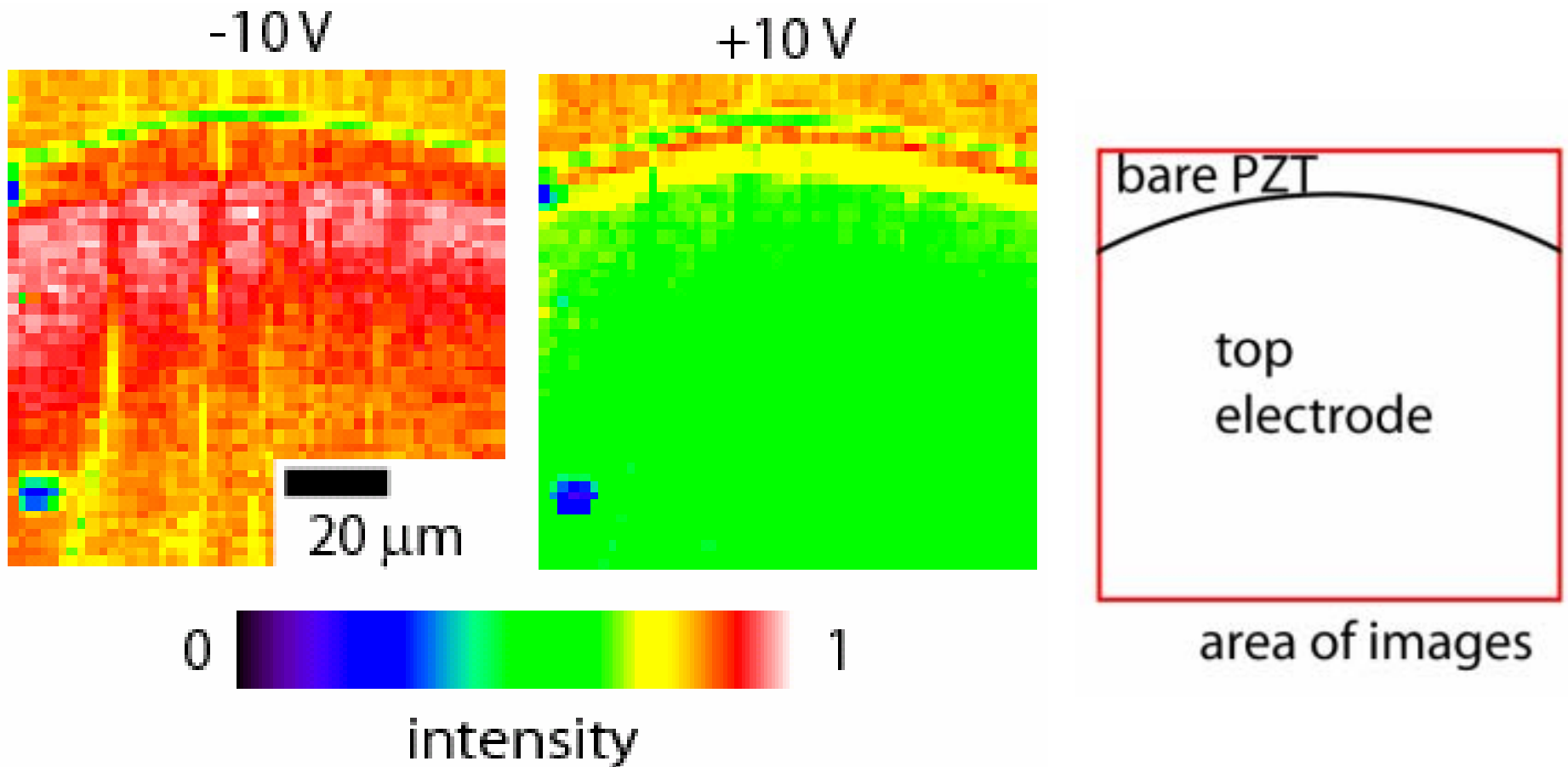


Limitations at Sector 7: Vibrations, Be Windows (?)

Probing Ferroelectric Polarization Switching with X-ray Microdiffraction

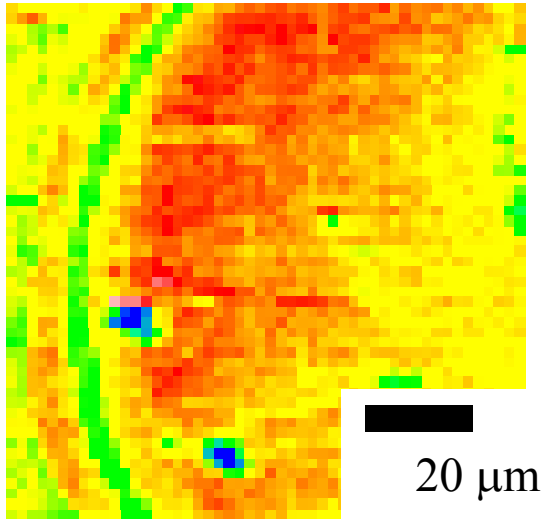


Imaging PZT Polarization Switching



Maps of the intensity of PZT (002) reflection vs. the position of the beam on the sample.
Intensity following $-10\ \text{V}$ pulse is 25% higher than

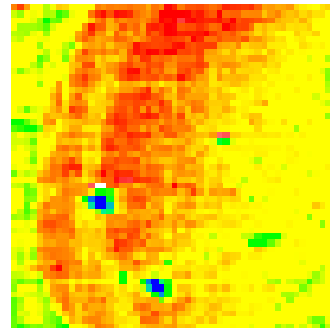
Switching with $E \approx E_c$



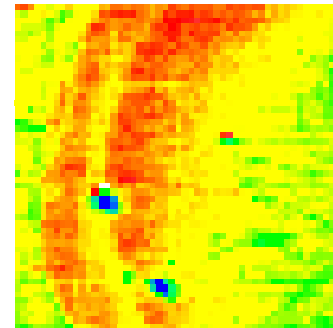
-10V

1. Apply negative voltage pulse to produce uniform polarization.

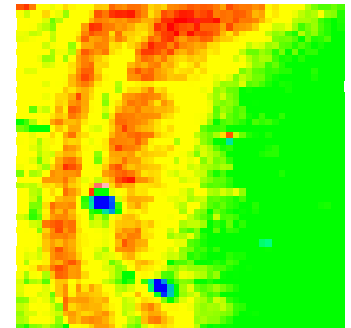
500 μs triangle pulses



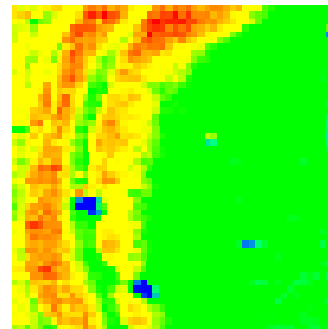
0.8V



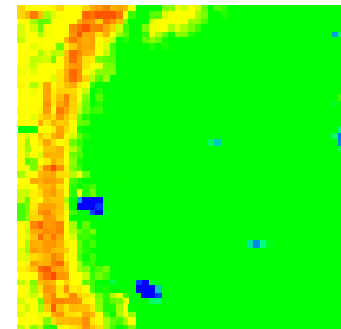
1.2V



1.6V



2.0V

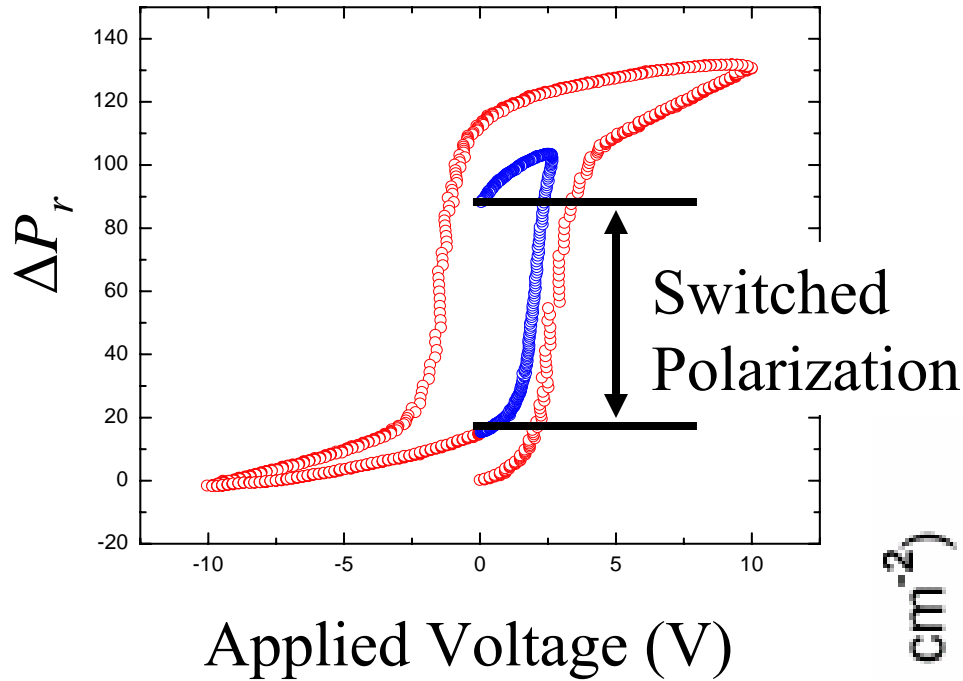


2.8V

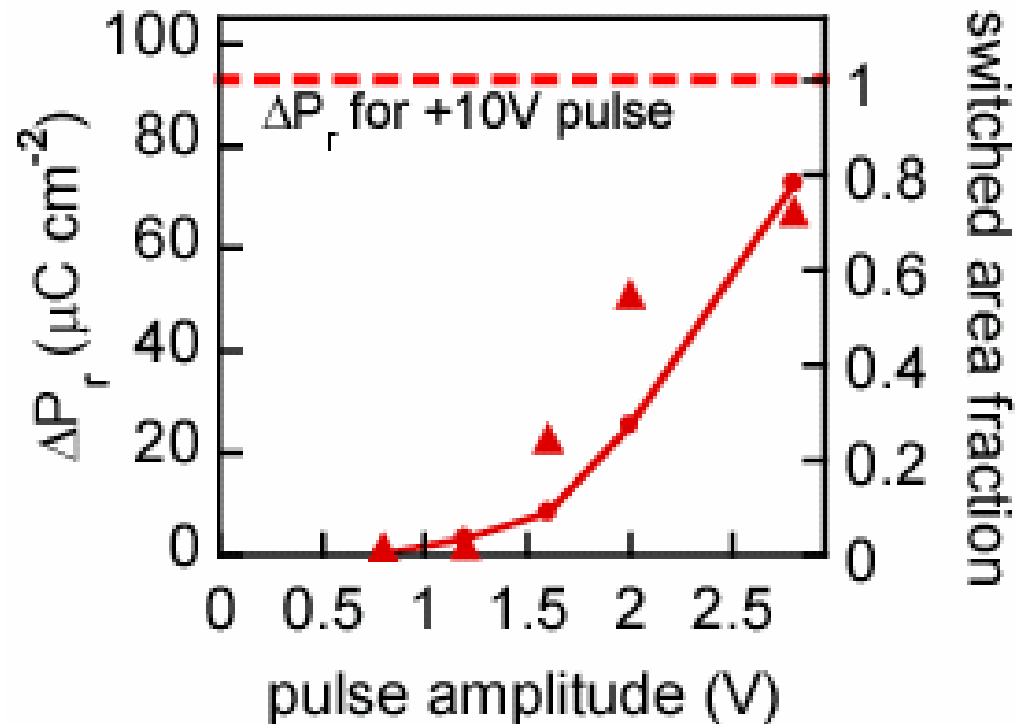
2. Apply a positive pulse near E_c .

Device switches in well defined areas.

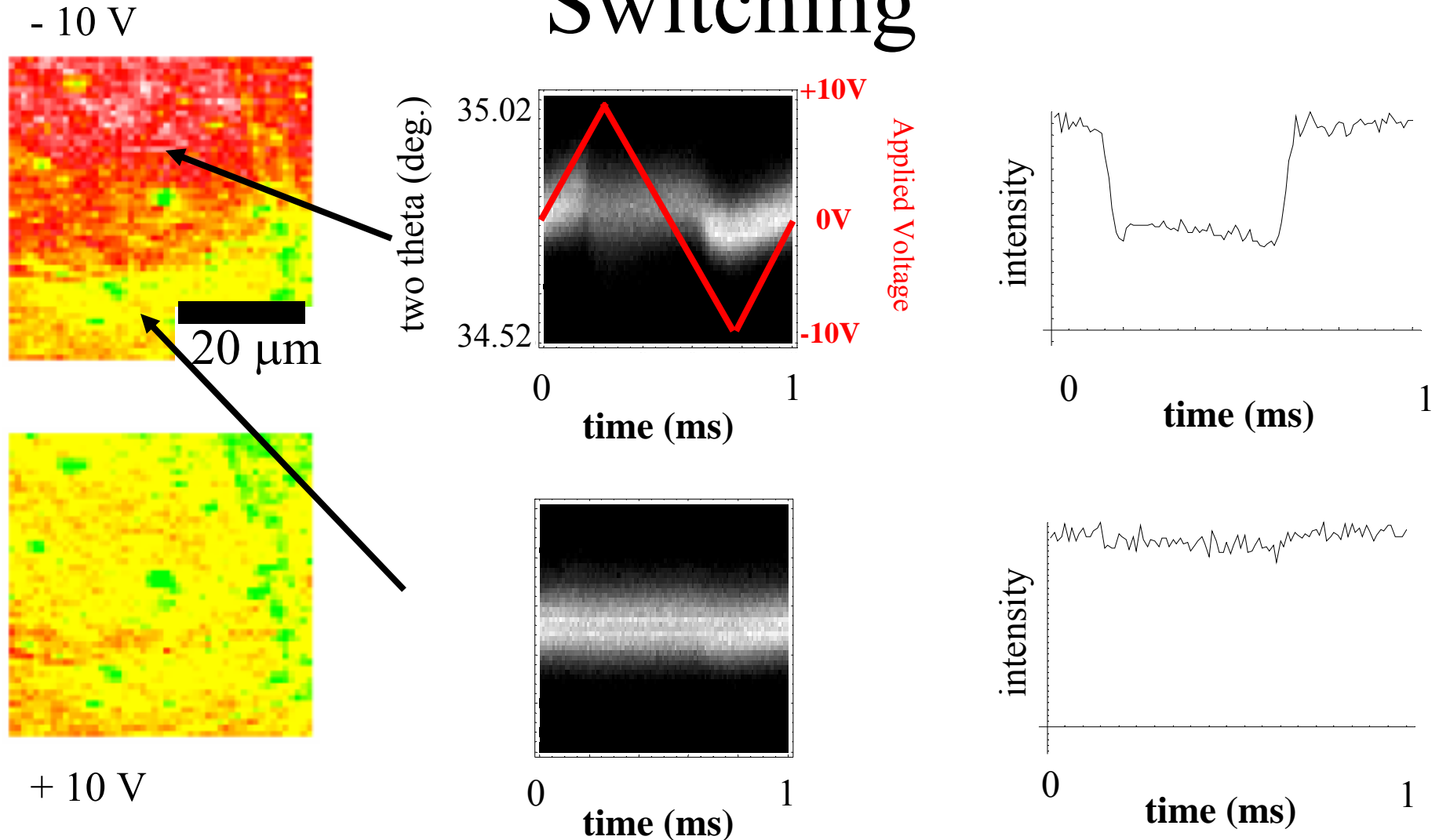
Quantitative Relationship of Polarization to Switched Area



Switched Area Measured from X-ray Microdiffraction Maps is Proportional to the Total Switched Polarization.



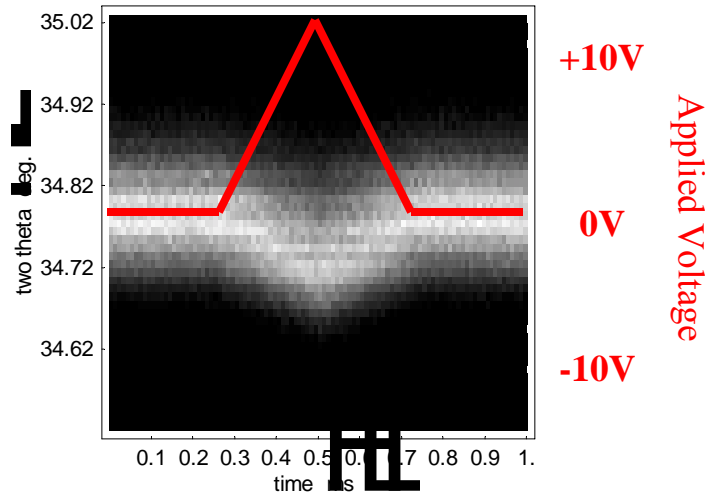
Time Resolved Diffraction During Switching



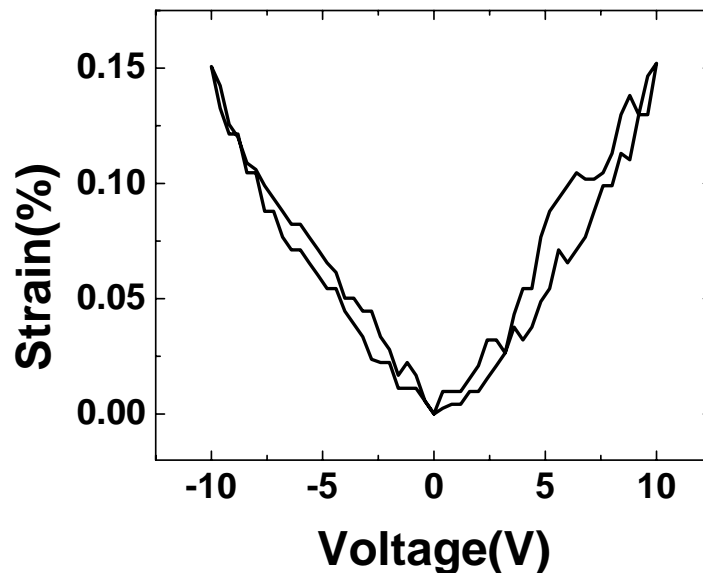
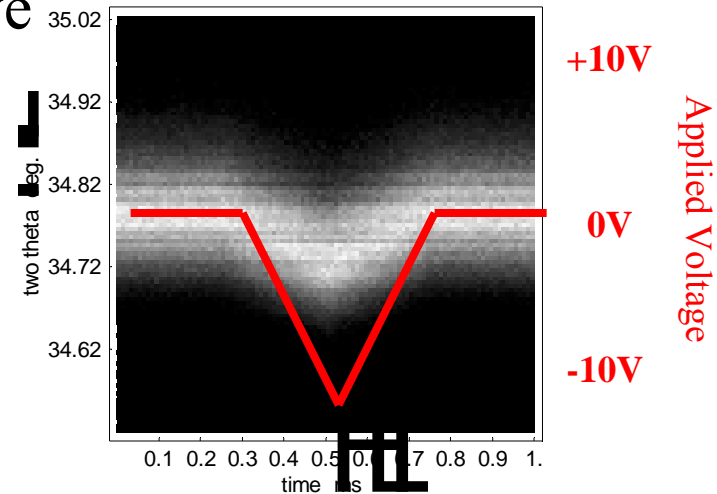
Switching of 200 μm diameter device limited by RC time constant.

Quantitative Measurement of Piezoelectric Distortion

Positive pulses



Negative pulses

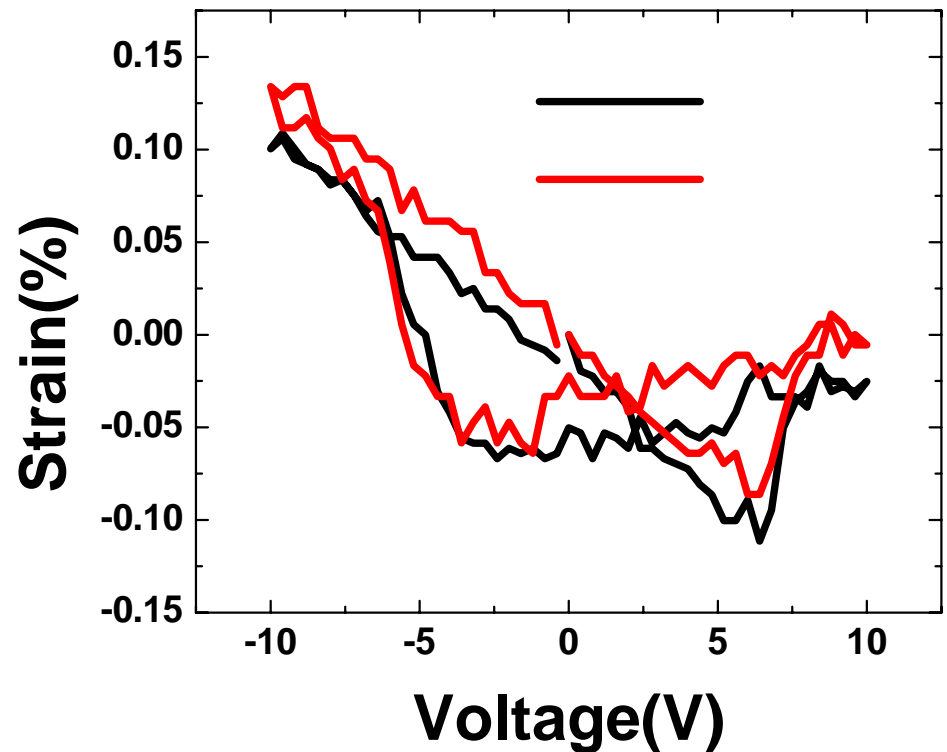
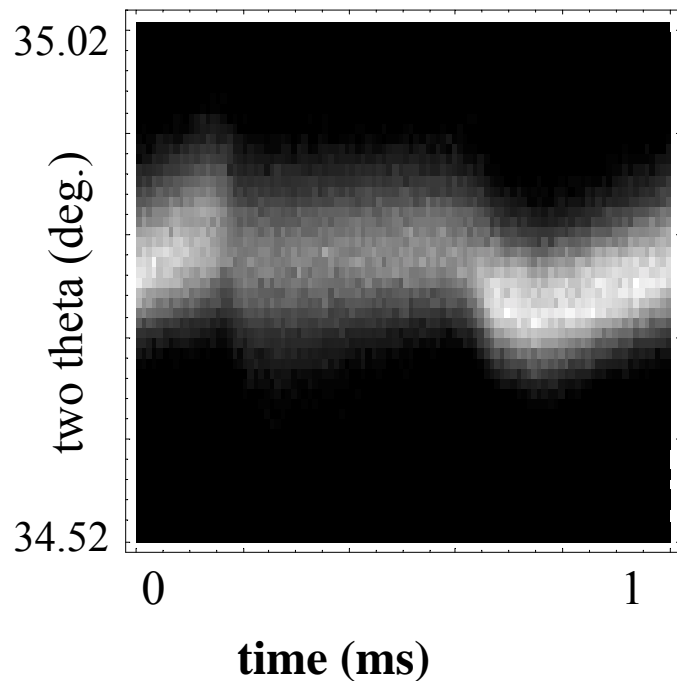


Both polarizations have $d_{33}=60 \text{ pm V}^{-1}$.

Quantitative measurement: Requires No Standards.

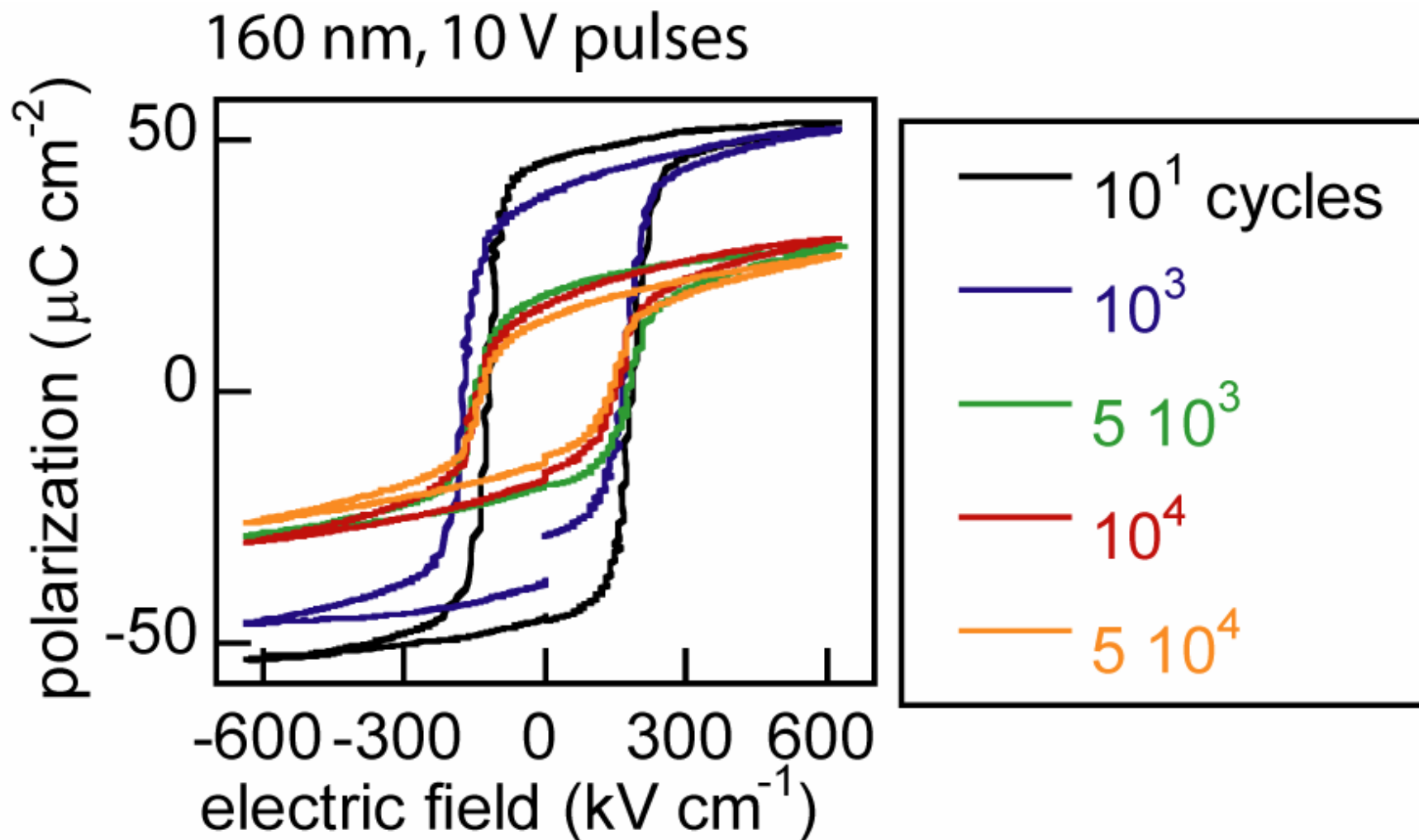
An Electromechanical Puzzle

During switching experiments the piezoelectric coefficients for positive and negative polarizations are different.

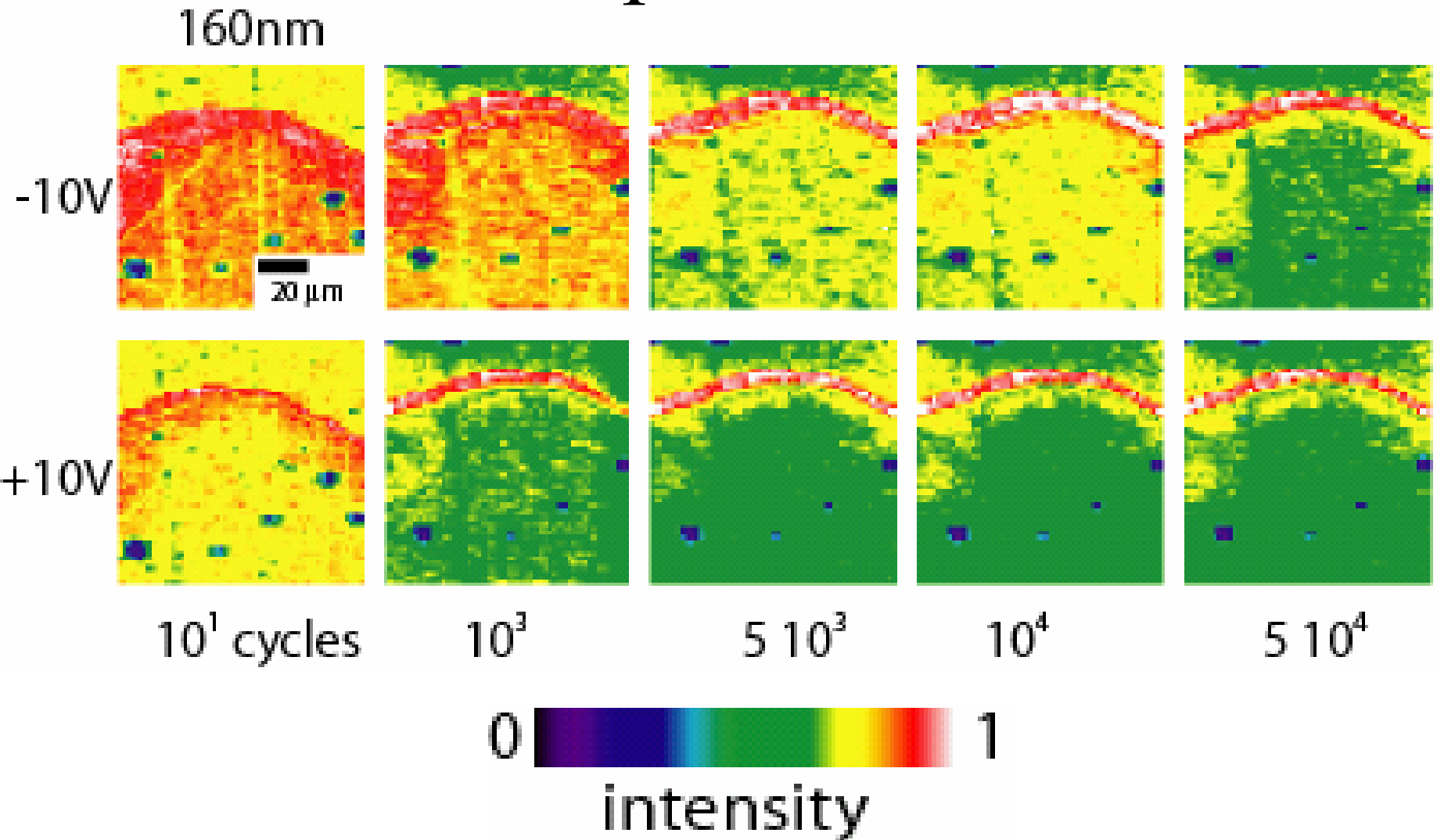


We think: Difference between top and bottom contacts.

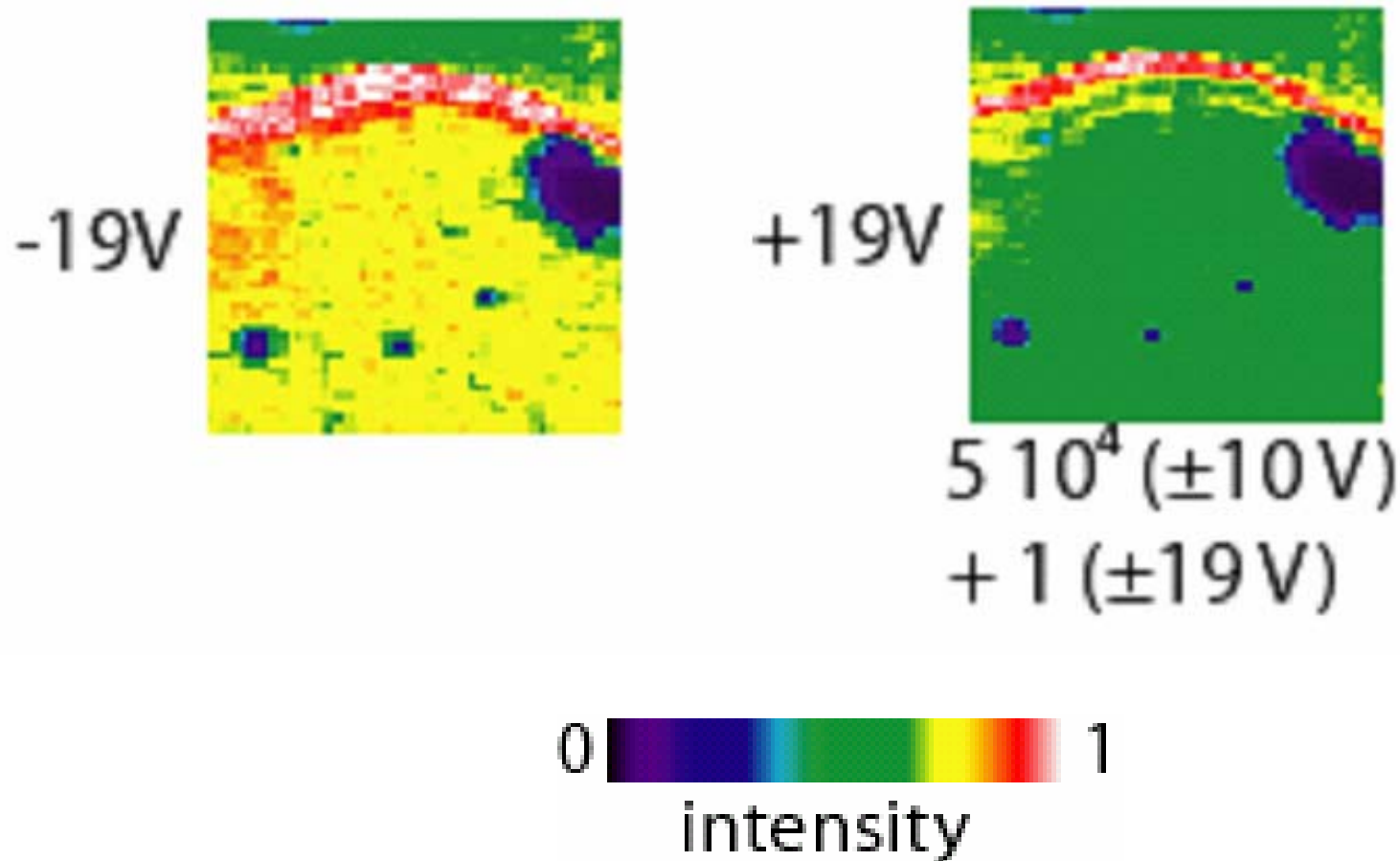
Polarization Fatigue



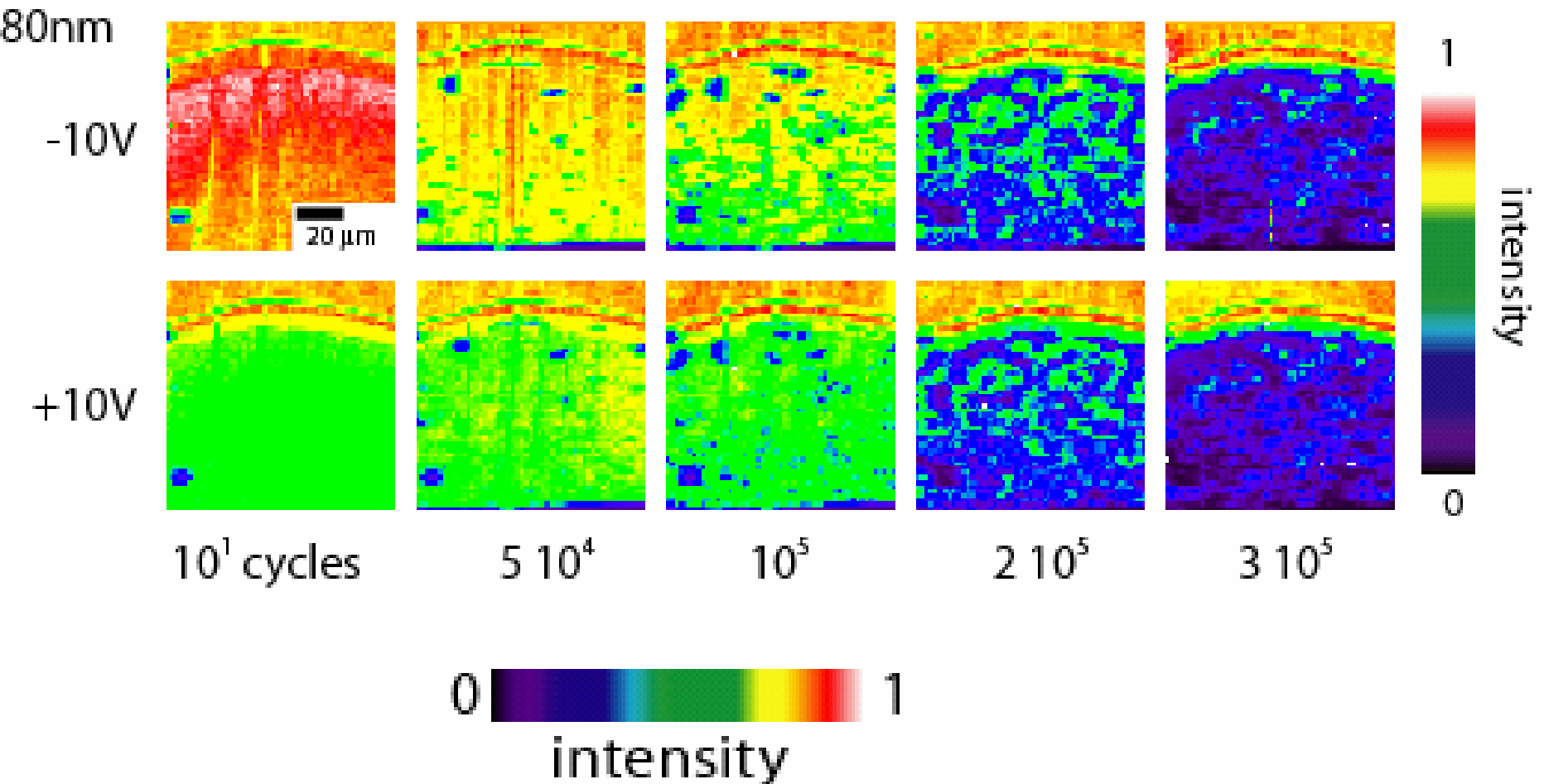
Polarization Fatigue: 160 nm, ± 10 V pulses



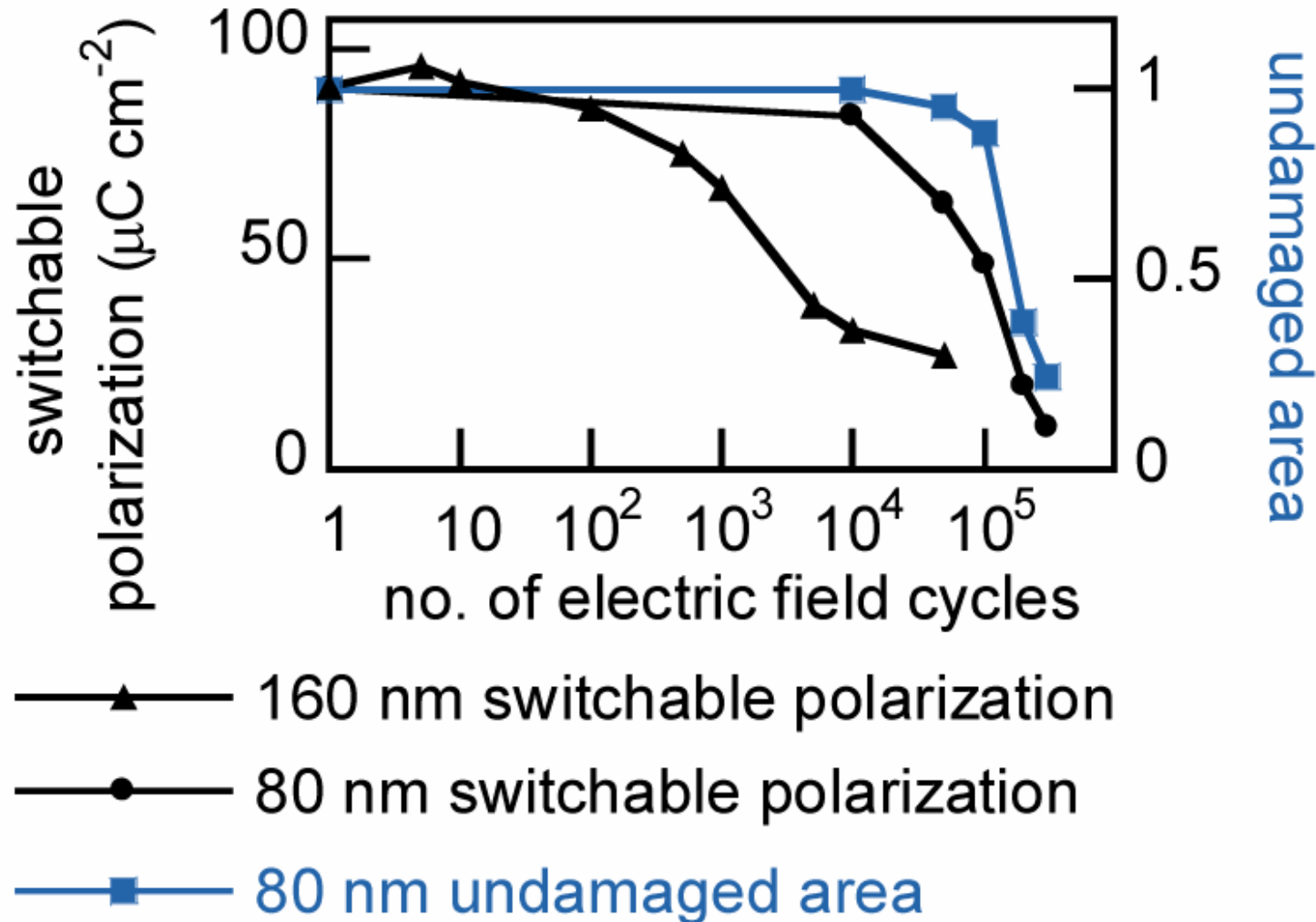
Higher Electric Field Pulses Partially Restore the Switchable Polarization



Polarization Fatigue at Higher Electric Fields



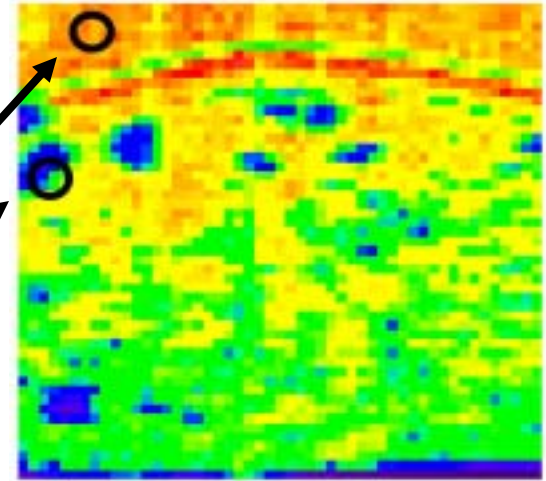
Polarization Fatigue at Higher Electric Fields



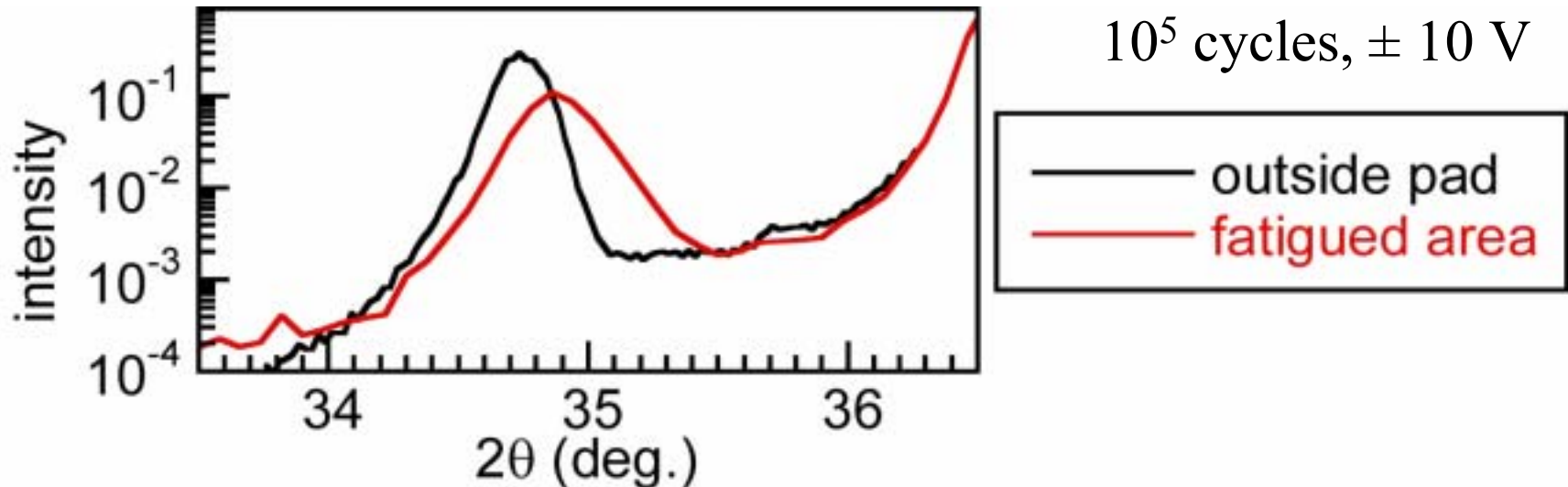
Structural Signature of Fatigue at High Electric Fields

Compare Structures at Points
Outside the Device With Areas
Fatigued at High Electric Fields

Theta-Two Theta Scans at Two Locations



80 nm thickness,
 10^5 cycles, ± 10 V



Conclusions: Ferroelectrics

Imaging

1. X-ray microdiffraction provides a new avenue to studying polarization switching in ferroelectric devices.
2. Quantitative agreement of x-ray observations with electrical measurements of switching.
3. Potential to take advantage of the flexibility of x-ray scattering techniques: resonant scattering, time resolved diffraction...

Fatigue

1. Fatigue in PZT devices with Pt electrodes pins the polarization in the state that would normally follow a positive voltage pulse to the bottom electrode.
2. Fatigue at **higher electric fields** in PZT thin films is accompanied by the gradual spread of a structurally distinct area.

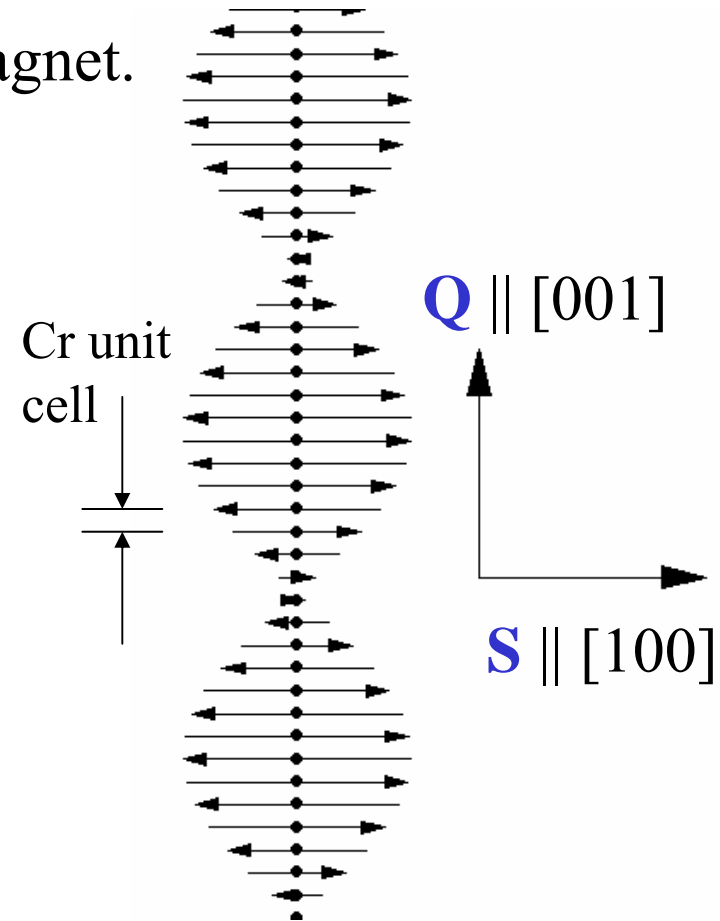
Spin density wave domains in chromium

Cr is a **spin density wave** (SDW) antiferromagnet.

- SDW leads to strain wave and charge density wave (CDW).
- Spins are **transverse** $T=123$ to 311 K, **longitudinal** for $T<123$ K.

Antiferromagnetic Domains:

- Modulation direction **Q** any $\langle 001 \rangle$
 \Rightarrow Three possible **Q** domains.
- Spin polarizations **S**, also $\langle 001 \rangle$
 \Rightarrow Two **S** domains in transverse phase.
 \Rightarrow Just one **S** ($\parallel \mathbf{Q}$) in longitudinal phase.
- Domains are responsible for macroscopically observable magnetic, mechanical, electrical phenomena.
- Previous domain imaging experiments are at the 1 mm scale.



Fermi surface nesting in Cr

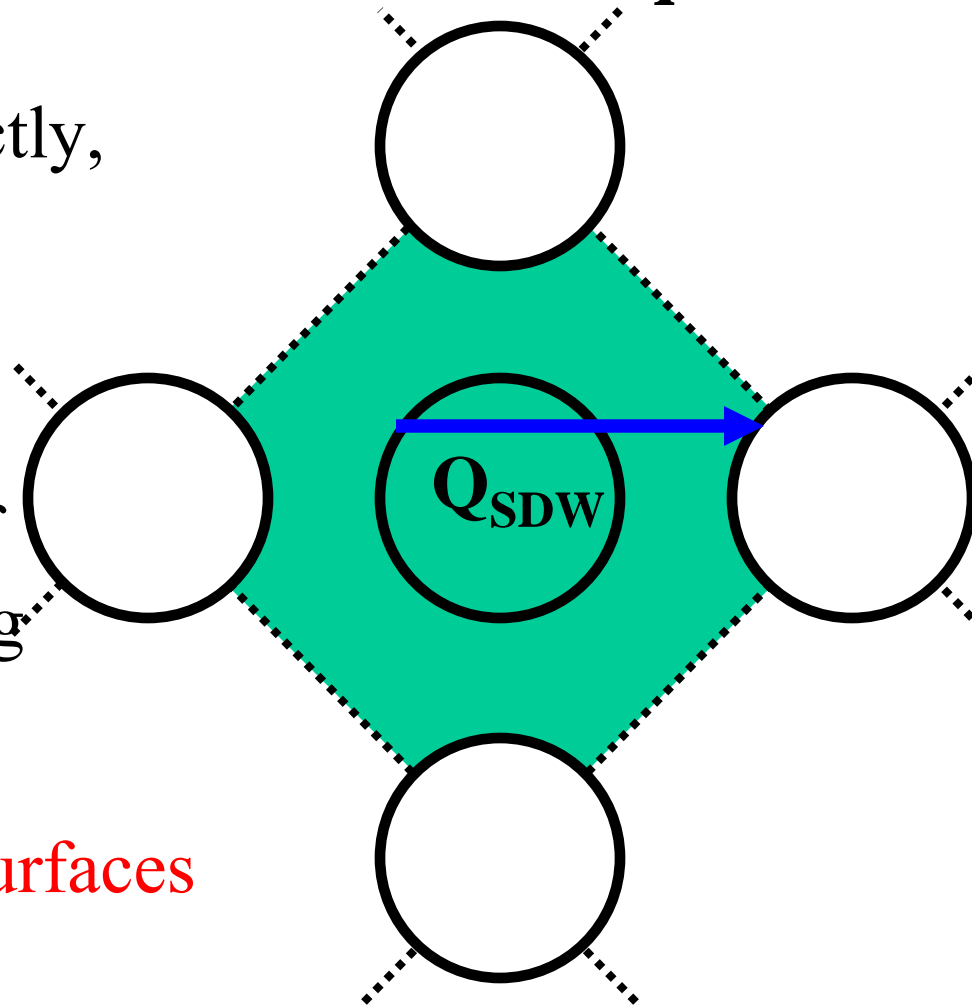
$\chi(\mathbf{q})$ susceptibility, response of hypothetical non-magnetic system to magnetic perturbation with wavevector \mathbf{q}

Difficult to calculate $\chi(\mathbf{q})$ directly, but common feature is

$$\chi(\mathbf{q}) \propto \sum_{\mathbf{K}} \frac{1}{E_{\mathbf{K}+\mathbf{q}} - E_{\mathbf{K}}}$$

where $E_{\mathbf{K}+\mathbf{q}}$ and $E_{\mathbf{K}}$ are pairs of filled and empty states differing in wavevector by \mathbf{q} .

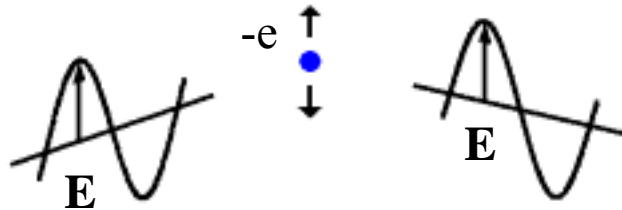
Band structure of Cr: Fermi surfaces nest with $\mathbf{Q}=(0,0,1-\delta)$, incommensurate with lattice.



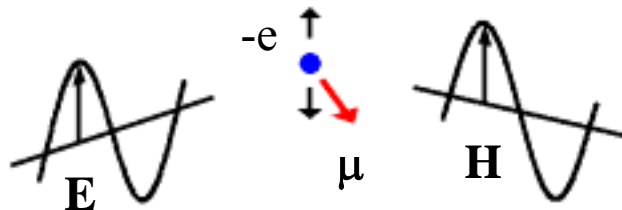
(Non-Resonant) Magnetic X-ray Scattering: Classical Picture

Force

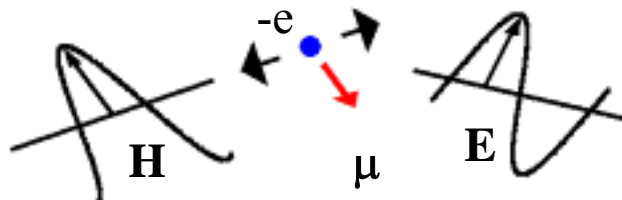
$$-e\mathbf{E}$$



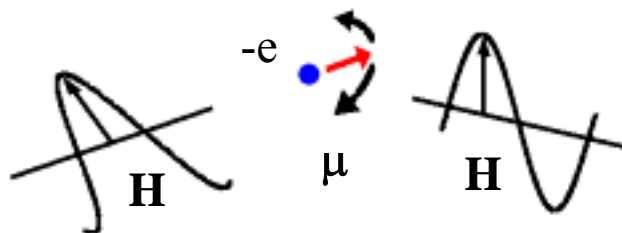
$$-e\mathbf{E}$$



$$\nabla(\boldsymbol{\mu} \cdot \mathbf{H})$$



$$\mathbf{H} \times \boldsymbol{\mu}$$



Radiation

electric dipole

“Thomson scattering”

magnetic quadrupole

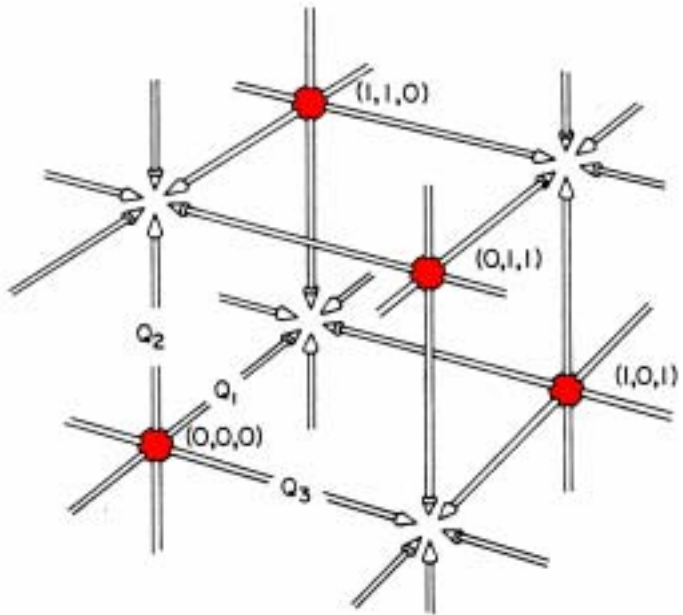
electric dipole

magnetic dipole

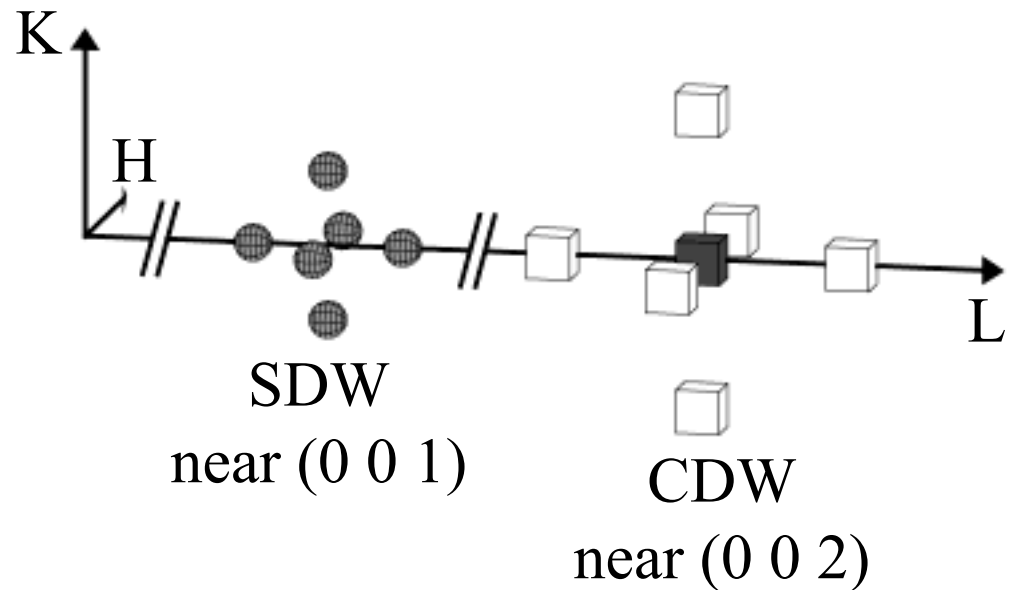
After F. de Bergevin and M. Brunel, Acta Cryst. A **37** 314 (1981).

Cr in reciprocal space

Magnetic scattering appears near forbidden lattice reflections.



Also: Strain wave (CDW) reflections near allowed lattice reflections.

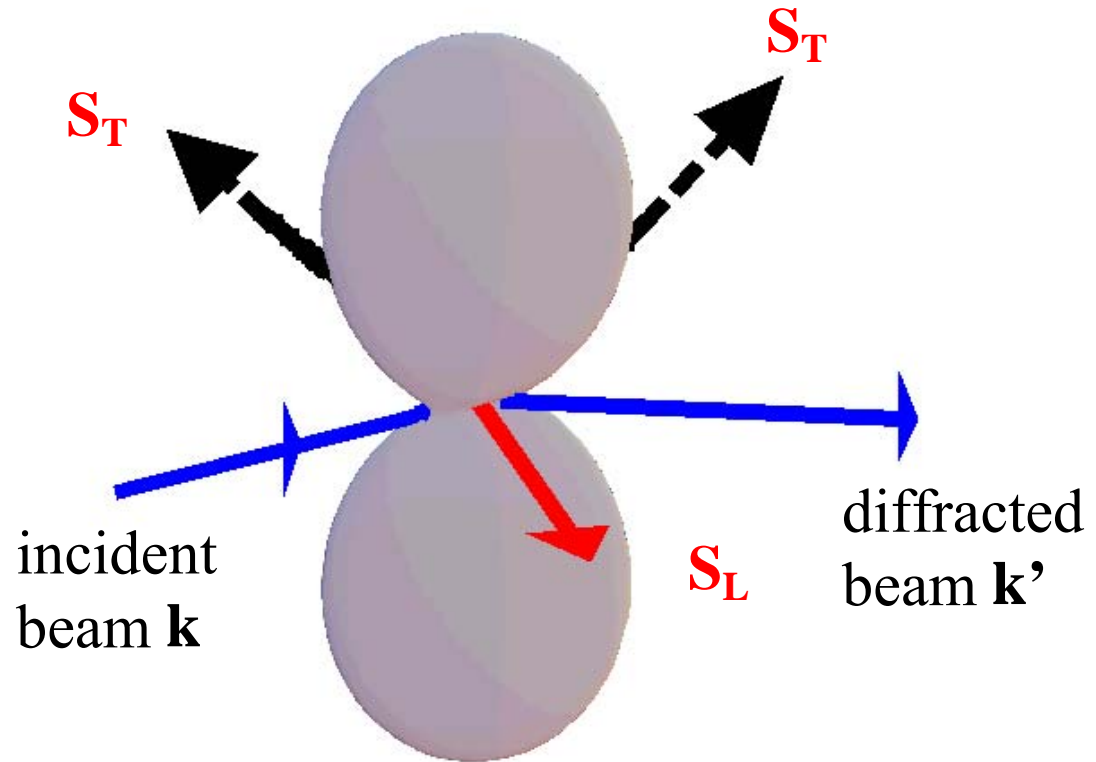


Form images using **either** type of reflection.

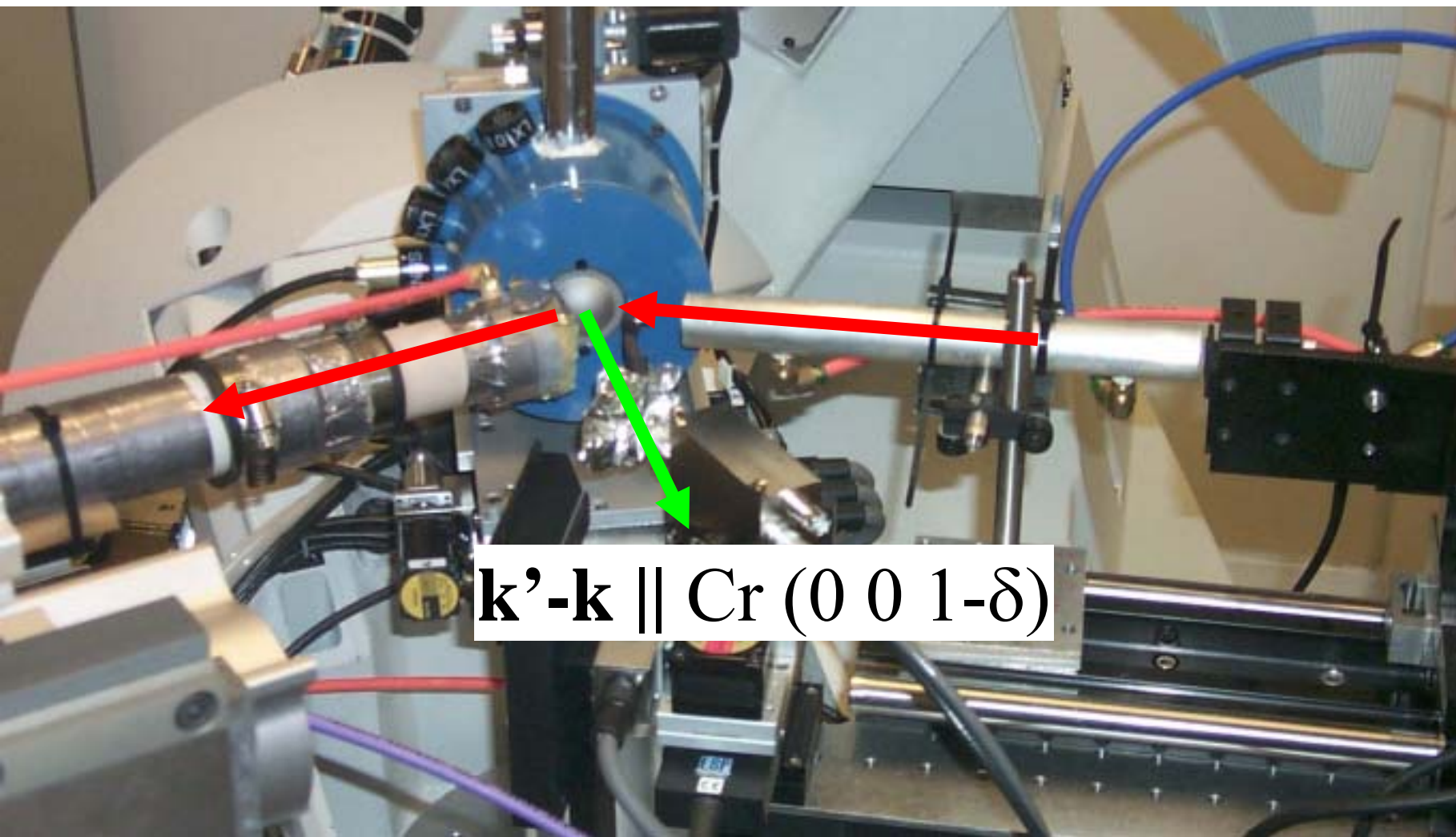
Non-resonant magnetic x-ray diffraction from Cr

Most important term of cross section scales as:

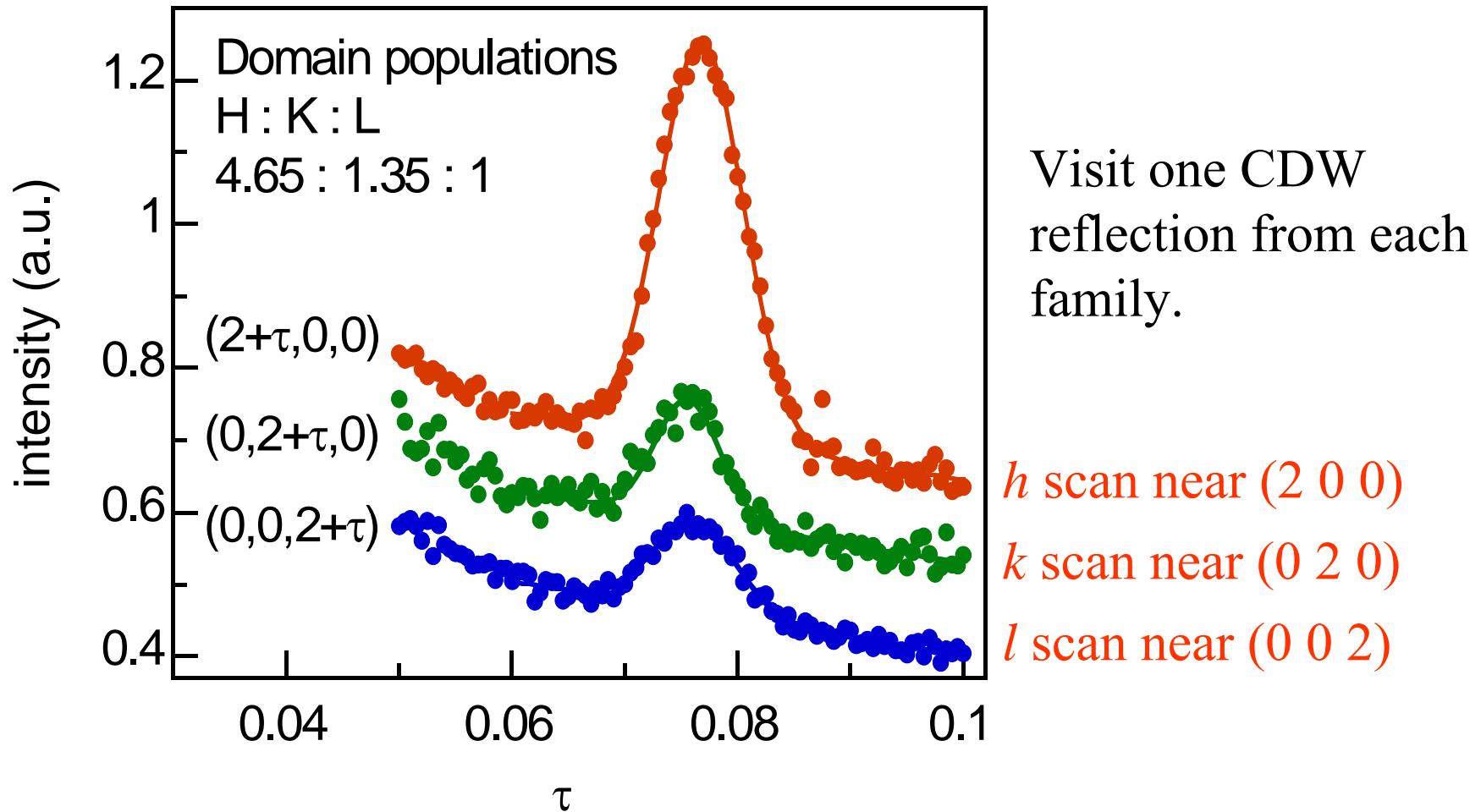
$$\left| \mathbf{S} \cdot (\hat{\mathbf{k}} \times \hat{\mathbf{k}}') \right|^2$$



Polar plot of cross section as a function of spin direction for a $\mathbf{Q} \parallel (001)$ domain in our geometry.



All three **Q** domains are present

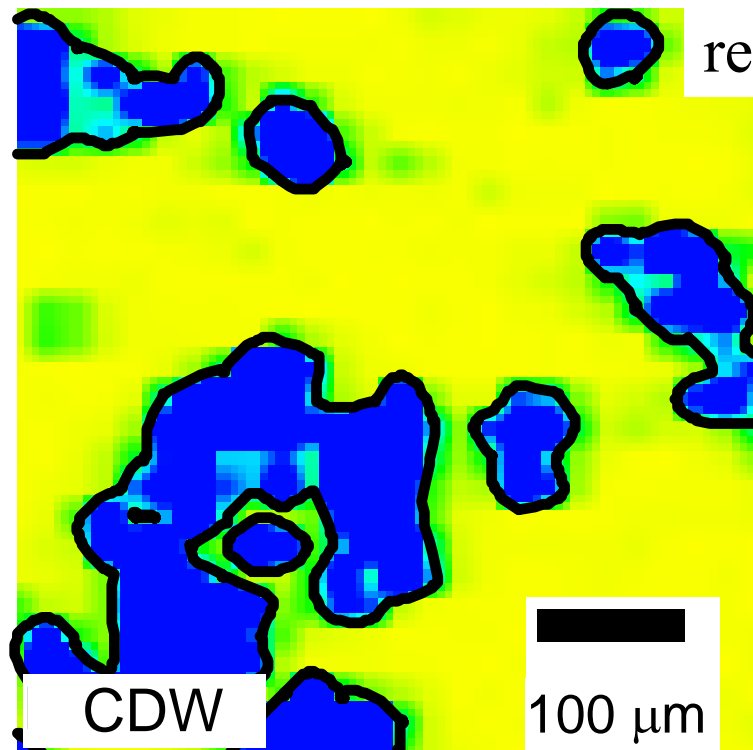
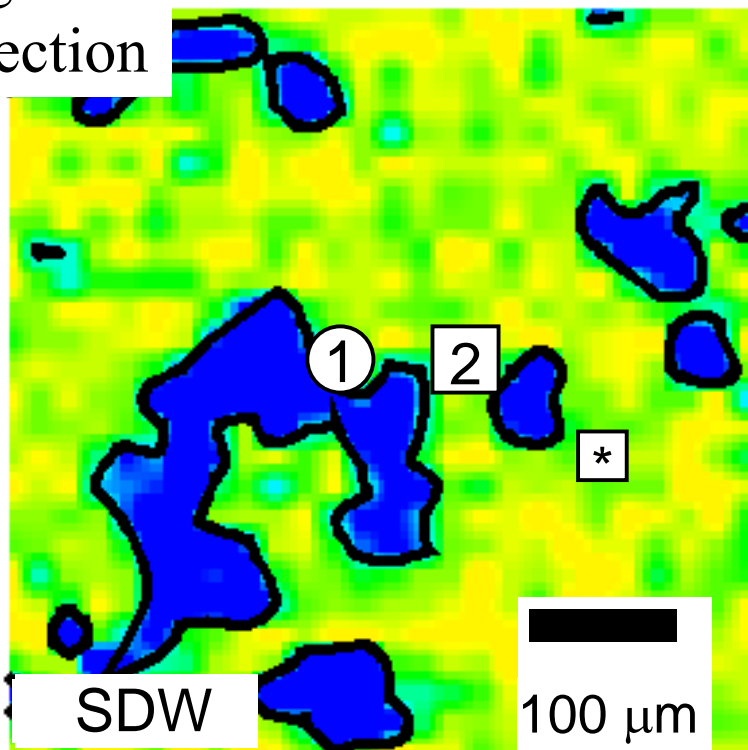


Room temperature laboratory diffractometer scans
with large mm-scale beam.

SDW Domains at 130 K

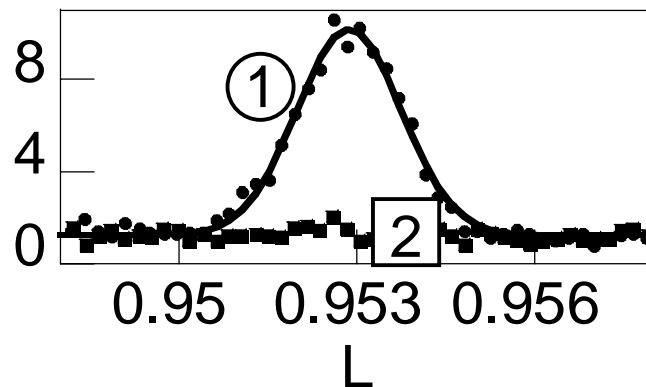
SDW
magnetic
reflection

CDW
charged
reflection



incident
beam
 $h\nu=5.8\text{ keV}$

SDW
intensity
 counts s^{-1}



incident
beam
 $h\nu=11.6\text{ keV}$

Spin-flip transition

Transverse SDW phase

Longitudinal SDW phase

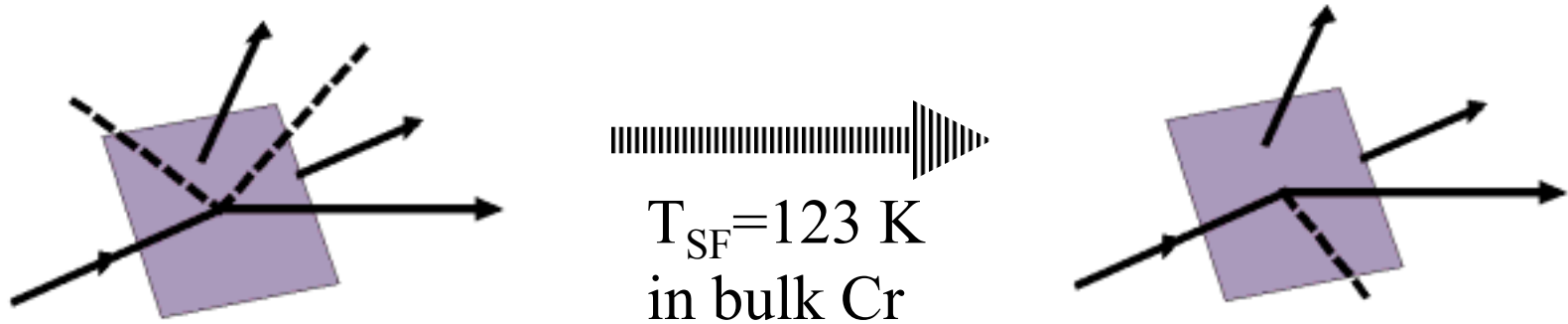
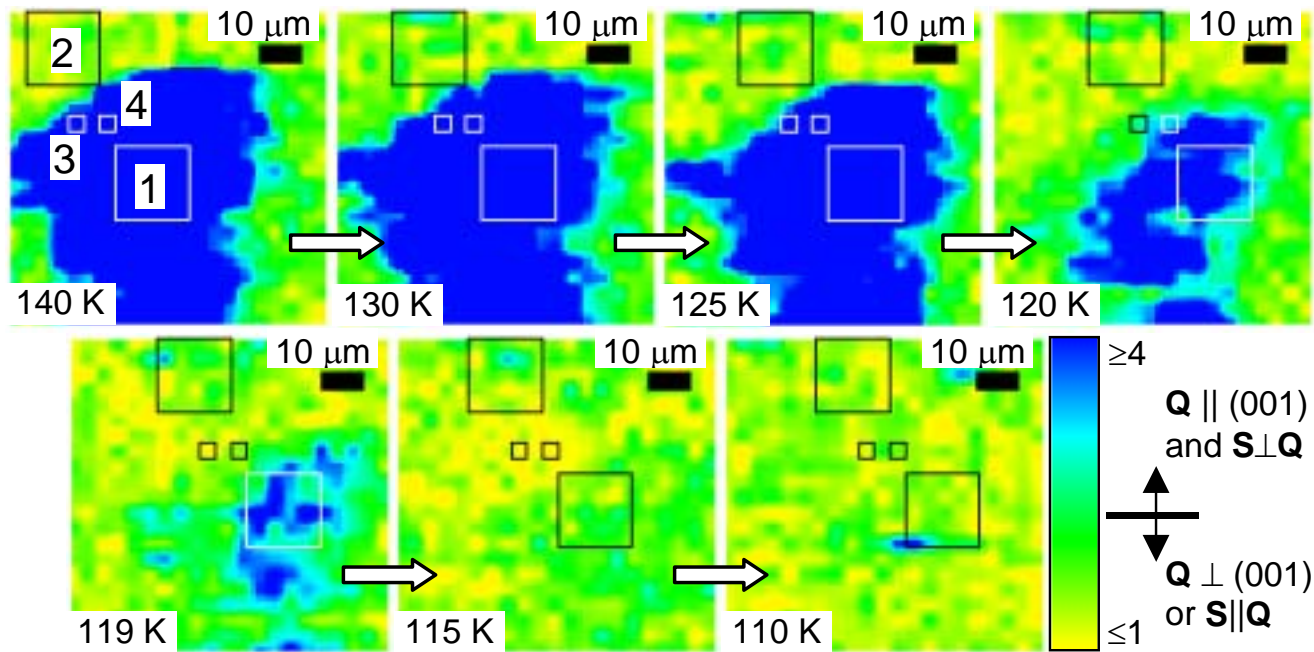


Image SDW reflection as a function of temperature.



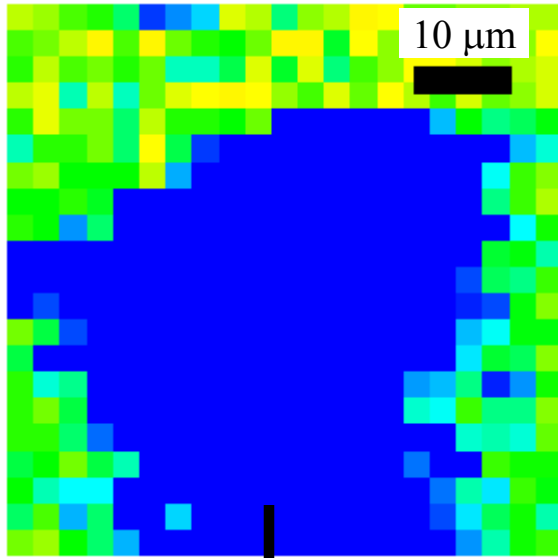
Magnetic reflection disappears!

Repeat with charged CDW reflection

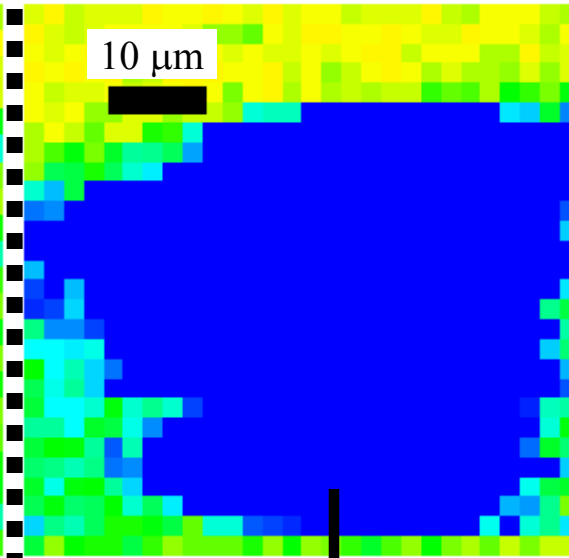
SDW **Magnetic** reflection

CDW **Charged** reflection

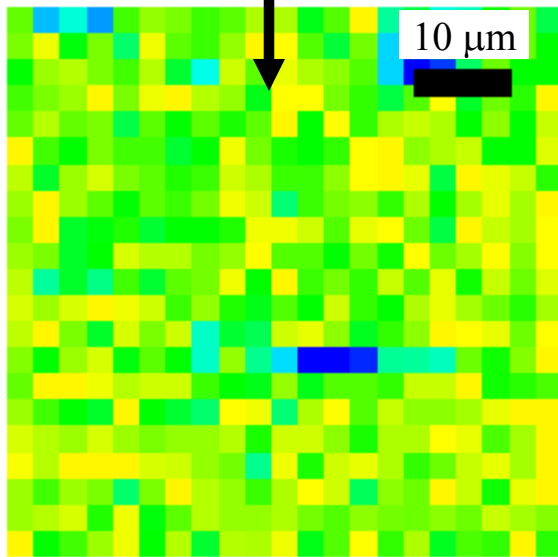
T=130 K



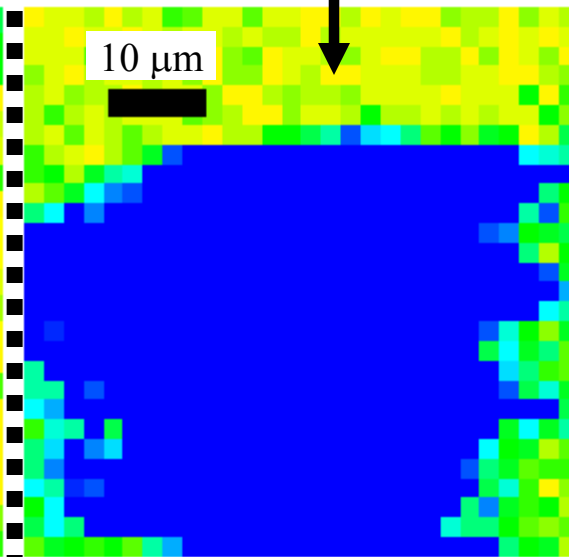
T=130 K



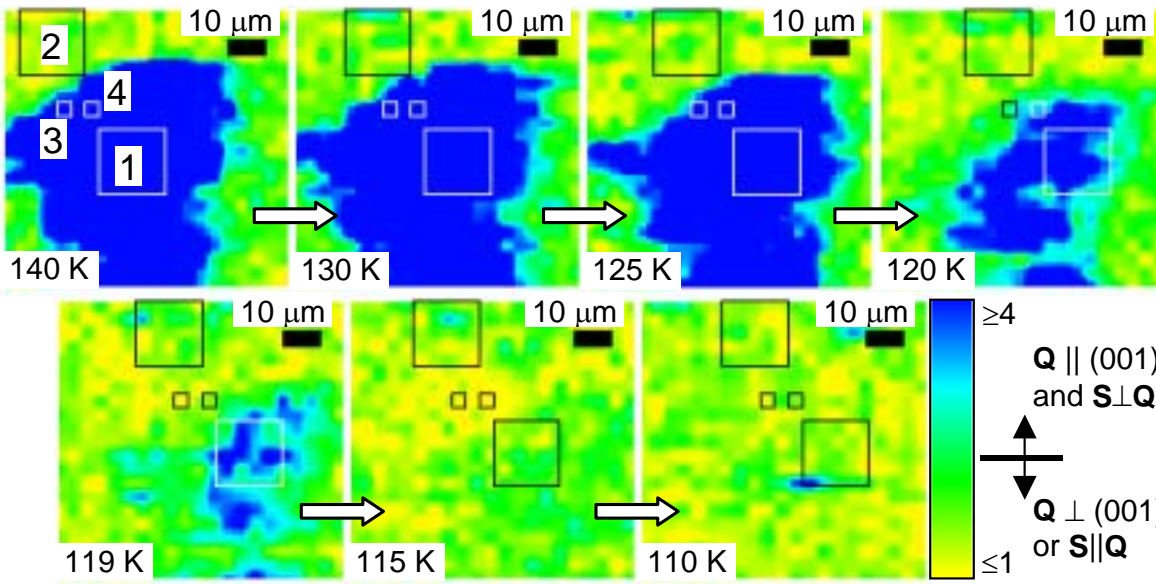
T=110 K



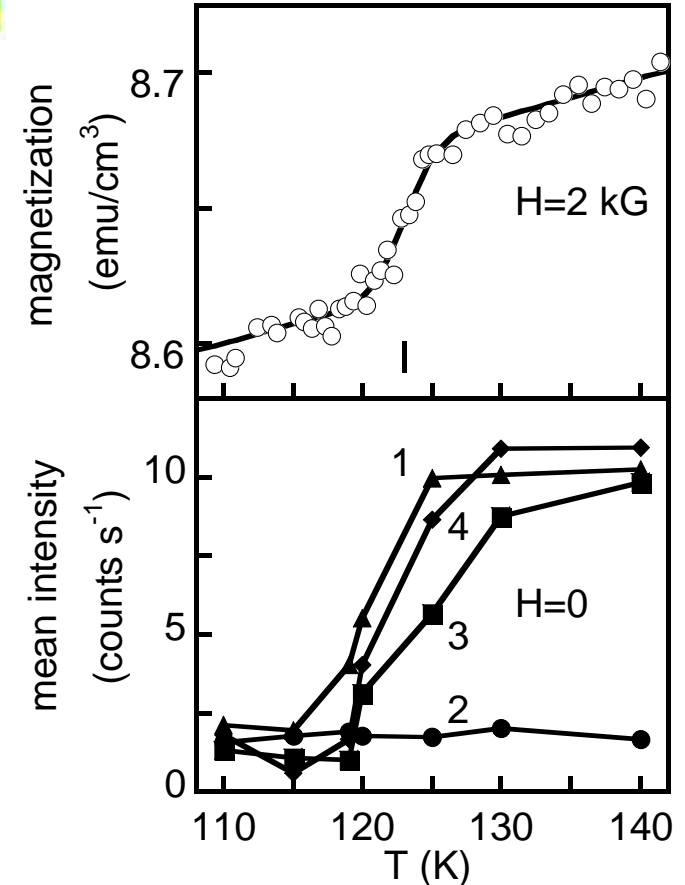
T=110 K



Spin flip transition begins at **Q** domain edges

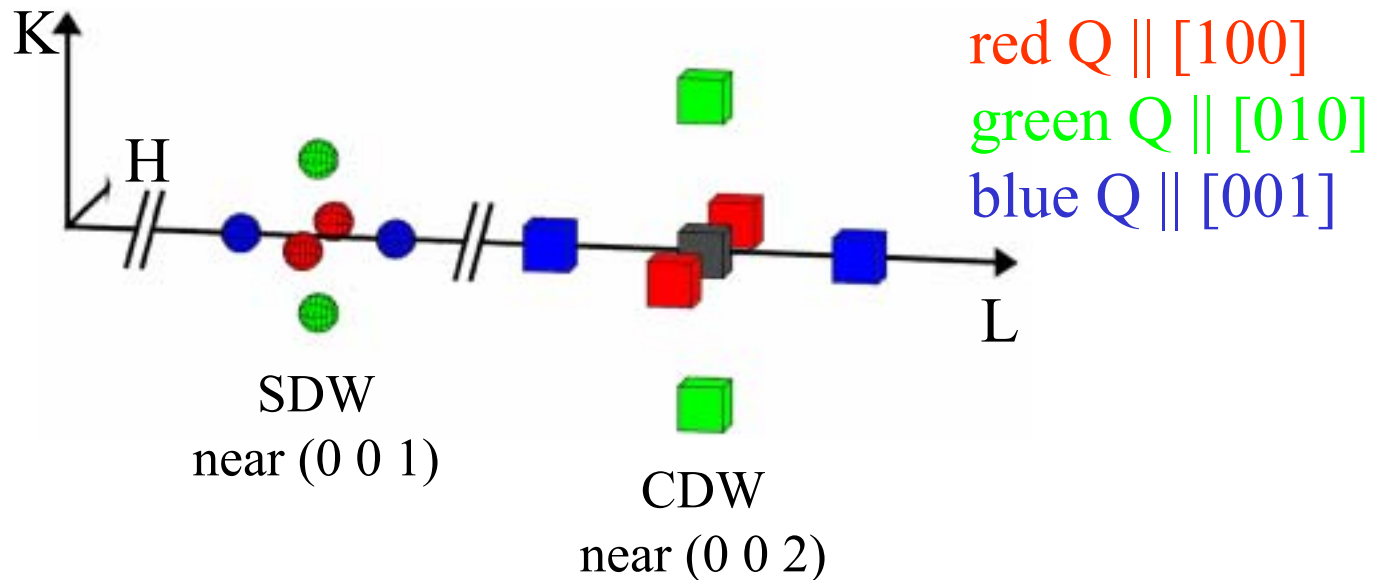


Nominally first order transition is broadened by several degrees, even at micron scale.



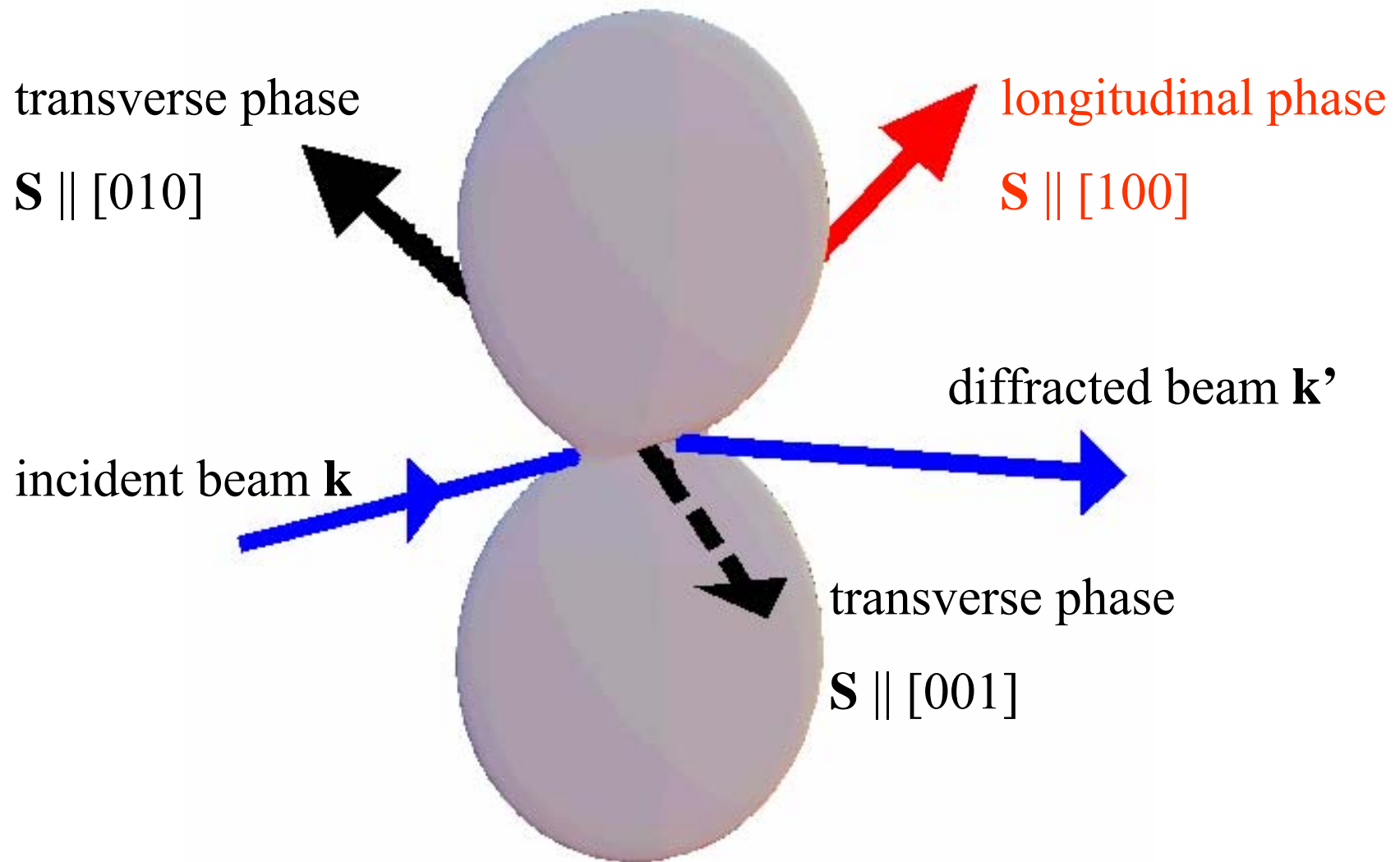
Learning more about domain walls

1) So far we've looked at $\mathbf{Q} \parallel [001]$.
What happens in neighboring \mathbf{Q} domains?



2) Two spin polarizations within transverse phase.

Magnetic cross sections in a $\mathbf{Q} \parallel [100]$ domain

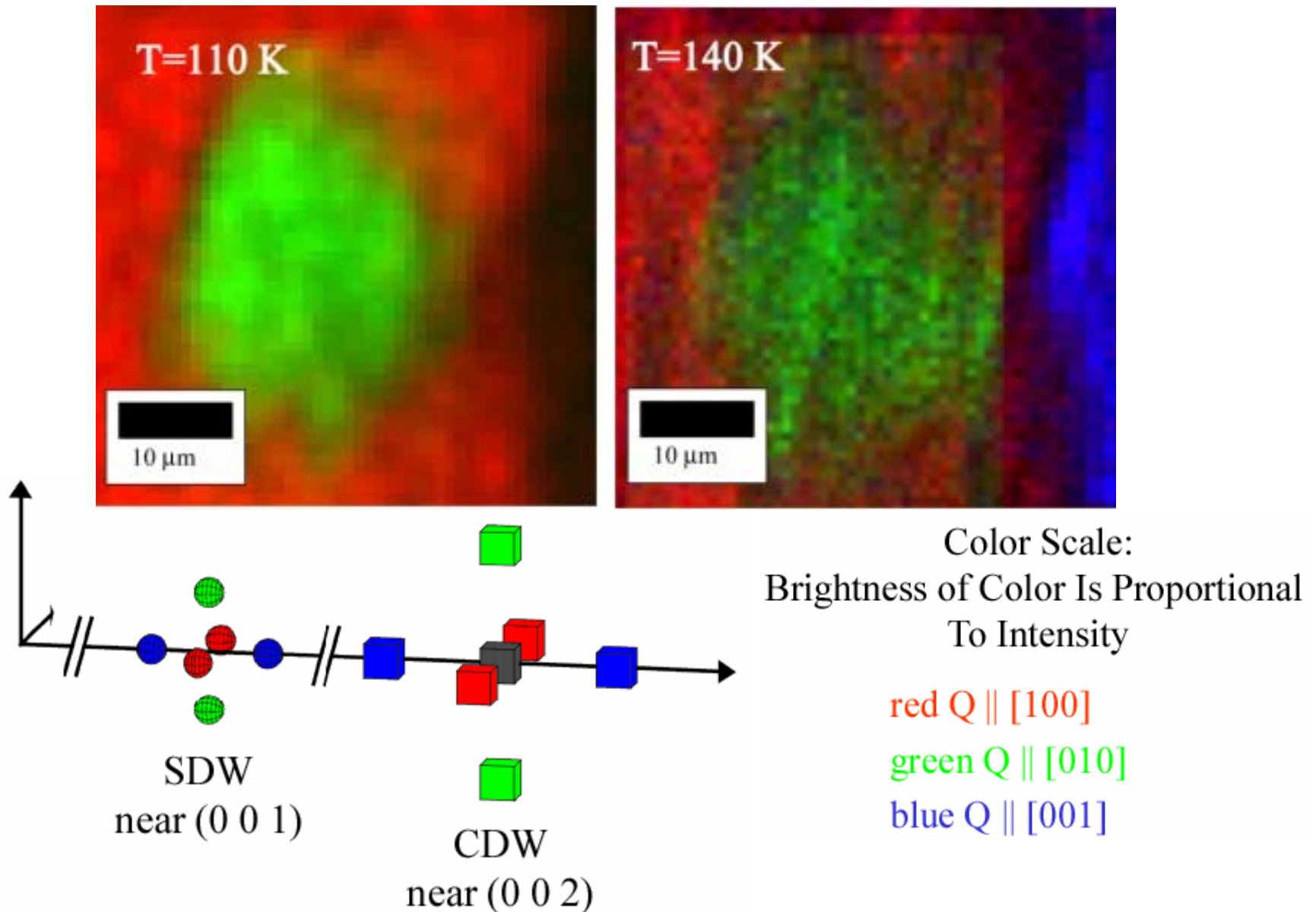


Cross section with \mathbf{S} along $[100]$ or $[010]$ than along $[001]$.

Selection Rule Summary

	H Domains ($\pm\delta$ 0 1) reflections	K Domains (0 $\pm\delta$ 1) reflections	L Domains (0 0 1 $\pm\delta$) reflections
Transverse Phase ($T > 123$ K)	Visible only in areas with S along K direction	Visible only in areas with S along H direction	Visible for both S polarizations
Longitudinal Phase ($T < 123$ K)	Visible	Visible	Not Visible

Magnetic imaging of three domains



Conclusions: Chromium

- Self organized or artificial domains at small scales are key to macroscopic properties. Imaging is important.
- Spin flip transition in Cr begins at domain walls upon cooling.
- Future work in Cr:
 - Control of domain walls
 - Separation of bulk and interface effects

Conclusion

- Today: Cr antiferromagnetism and PZT ferroelectricity
- Future directions:
 - Coupling of strain between layers in multilayer films
 - Direct measurements of ferroelectric polarization domain wall velocity
 - Size effects in ferroelectric materials